We appreciate the generally favorable nature of the peer reviews and the opportunity to enhance the paper by responding to specific comments. Reviewer comments are in italics, with author's response provided below each corresponding comment. Note that line numbers in responses refer to the revised manuscript.

Response to RC1: Anonymous Referee #1:

1. *The first paragraph of Sect. 1 introduces the importance of N fertilizer on agricultural land and its implication on N emissions, but neglected those from non-cultivated land. In addition, it is not clear why only NO and NO_2 emissions are mentioned in this paragraph, and their relationships. Merging this part with the third paragraph might improve the logic here.*

> We address the importance of soil nitrogen emissions from non-cultivated (non-agricultural) land in the second paragraph of Section 1 (Lines 50-53):
>
> "Recent studies have shown higher soil NO_x even in non-agricultural areas like forests to significantly impact summertime ozone in CONUS (Hickman et al., 2010; Travis et al., 2016). Consequently, it is increasingly important to estimate both N fertilizer-induced and non-agricultural NH_3 and NO_x emissions in air quality models."
>
> We adopt the reviewer's suggestion to improve the logic of the flow in the third paragraph (Lines 54-58):
>
> "Soil NO emissions tend to peak in the summertime, when they can contribute from 15-40% of total tropospheric NO_2 column in the continental U.S. (CONUS) (Williams et al., 1992; Hudman et al., 2012; Rasool et al., 2016). Summer is also the peak season for ozone concentrations (Cooper et al., 2014; Strode et al., 2015) and the time when photochemistry is most sensitive to NO_x (Simon et al., 2014)."

2. *L79: the impacts of N_2O emissions are not introduced as that for NO_x, NH_3, and HONO.*

> We add the following statement in Line 71:

“Soils and agriculture are the leading emitters of N_2O, a potent greenhouse gas (IPCC, 2013).”

3. *L223: it is a little confusing on the different versions of CMAQ and the schemes of NO emission in these versions. For example, is YL or BEIS used in CMAQ? In which version. This confusing issue can also be found in later of the manuscript due to too many schemes, methods, interaction systems, datasets are introduced here. A clarification of the abbreviations and the purpose of them could be useful to readers.*

To clarify ‘CMAQ-YL’ (in Line 224) refers to the original CMAQ v5.1 which has the Yienger and Levy (1995) (abbreviated as YL) scheme for soil NO estimation used in the Biogenic Emission Inventory System (BEIS) for in-line biogenic emissions calculation in CMAQ. The term ‘CMAQ-YL’ term was used to highlight that CMAQ’s default soil scheme differs slightly from the original scheme presented by Yienger and Levy (1995) (refer to section 2.1, Lines 216-241). To further avoid confusion, we added in Line 239:

“However, for sake of simplicity we refer to ‘CMAQ-YL’ merely as ‘YL’.”

The only other two variations to this original CMAQ v5.1 code are the replacement of YL in the in-line BEIS with:

a) ‘BDSNP’ (earlier implemented in previous version of CMAQ i.e. v5.0.2 presented in Rasool et al. (2016) and updated for v5.1 for this paper), and

b) The new ‘Mechanistic’ (or ‘Mech.’) scheme implemented in CMAQ v5.1 and presented in this paper for the first time.

Fig. 1, Section 2.1, Tables 1 and 2 clearly described and distinguished these three variations for soil N estimation in CMAQ v5.1 (CMAQ-YL or ‘YL’ actually being the original implementation of CMAQ v5.1 available in CMAQ’s official distribution from U.S. EPA). In addition, results presented in the paper are compared between these three different schemes.

4. *Similar to points 3, Sect. 2.2 is a little hard to follow given different land covers are used and converted in different model.*

Table A2 gives the mapping of NLCD 40 land cover types to MODIS 24. Also, Table A1 gives the different climate zones in which the respective MODIS 24 land cover types fall. Our mechanistic scheme only uses NLCD 40 as it is the default land cover definition used in CMAQ. NLCD 40 to MODIS 24 conversion was needed only in BDSNP as it used constant soil NO emission factors related to non-agricultural land covers (classified as per MODIS 24 nomenclature), which have also been described in Rasool et al. (2016).

5. *Sect. 2.6, the mechanisms are very well organized and presented. But it could be better whenever the factors impacting concentrations or fluxes can be referenced (e.g., fXXX in those equations).*

We actually do reference factors affecting soil nitrogen fluxes as ‘fXXX’ (generic form of function) in Equations 2-7 in Section 2.1 (Overview of Soil N schemes) for ‘YL’, ‘BDSNP’ and ‘Mech.’ schemes. These factors or functions (fXXX) are expanded in detail in different equations throughout Sections 2.5 and 2.6.

6. *The model comparison and evaluation are only conducted for two months in one year (May and July of 2011). It is crucial to explain the reasons in more detail. Readers may very curious about why. For example, why not using multi-month (e.g., for a whole year) and multi-year (e.g., 5-10 years) for evaluation? Is that due to the availability of observations? If so, it would be necessary to list the available observations. Unless using two months of a single year is well justified, it could be good to use more observations for seasonality, or even interannual variability, given that the purpose of a model (and the evaluation) is to be able to simulate spatio-temporal changes.*

The period between 1 May to 1 August has been established to exhibit ~ 2/3 of the total annual soil NO_x budget (Hudman et al., 2010). Hudman et al. (2012) also exhibited the soil NO_x to be maximal in the months of May (onset of growing season) and July (offset of growing season). Rasool et al. (2016) also established by running a standalone BDSNP soil NO parametrization for the whole year that May and July have the highest soil NO fluxes.

The observational studies giving maximum soil NO emission rates in Table 3 happen during May and July as well. Hence, for a computationally intensive, regional-scale (Continental US i.e., CONUS) simulation like ours that involved both EPIC and CMAQ, focusing on May and July makes sense based on the above justifications. For inter- and intra-annual variability, EPIC derived soil Nitrogen pools, other relevant soil properties, emission inventories and meteorology for different years are required, which is beyond the scope of this study.

7. *Sect. 2.8, what about the validation of N_2O emissions?*

We stated in Lines 647-649 in section 3.1, that:

"However, unlike NO_x emissions, for N_2O no background conditions or emission inventory is in place in CMAQ's chemical transport model, so comparisons with ambient observations are not yet possible."

This highlights the need for further work within CMAQ to include greenhouse gases like N_2O, which are not accounted in its chemical transport model currently. The absence of background/initial conditions and an emissions inventory for other sources of N_2O resulted in our choice to keep N_2O as a separate diagnostic output of our emissions model rather than an input to chemical transport modeling.

8. *Sect. 3.1, it is not clear what is the anthropogenic emissions. Please define it? Whether emissions caused by fertilizer application are anthropogenic?*

We clarify that we were referring to anthropogenic fossil fuel emissions (Lines 621-623):

"However, the aggregated budget of soil NO is much less than anthropogenic NO_x from non-soil related sources, because fossil fuel use is concentrated in a limited number of urbanized and industrial locations."

9. *L630: when exactly the peak emissions happened in site observation? Are they also in May and July?*

Yes, as mentioned in response to RC1 comment #6: The observational studies giving maximal soil NO emission rates across different sites in Table 3 happen during May and July (onset and offset of growing season respectively). That is also a reason justifying the simulations during these months specifically, besides May and July also being the peak soil NO_x months in the year.

10. *L638: differences are obvious also in Canada. It may be good to explain this too.*

BDSNP estimates higher soil NO emissions than the other models in forested regions of northeastern Canada, like due to the higher emission factor that it assigns to forest biomes (Rasool et al., 2016). The mechanistic scheme estimates lower emissions there because it tracks the actual N transformation processes.

11. *Sect.3.2, Why not directly compare it with observations like in Fig. S2-b. It should be mentioned that negative bias in difference means less bias compared to observation. Statistics on the mean biases from different schemes are important, and should be presented. For example, the 1:1 scatter plot compared to observations, which may quantify the improvements and disadvantages.*

Our aim is to show the difference that results from using the 'BDSNP' and 'Mech.' schemes relative to original CMAQ (i.e. 'YL').

We added the following in Lines 673-674 as suggested by the reviewer:

"In addition, negative bias in difference means less bias compared to observation (Figures 6-10)."

We assert that spatial plots of statistics like Mean Bias are preferable to scatter plots because they represent spatial patterns in model performance.

12. *Fig.10: mechanistic scheme is worse compare to that of YL in northeast US. Can it be explained?*

Mechanistic scheme estimates for total NO_x are lower than those from YL in northeast US, as evident in Figure 5. That explains the higher positive bias in $PM_{2.5}$ NO_3 in Mechanistic scheme compared to YL with respect to the observation in Figure 10. This underestimation may be attributed to lack of excess manure N that is applied to agricultural filed in vicinity of animal feedlots while estimating soil N in EPIC (also described in Lines 719-727). Additionally, EPIC optimizes the fertilizer application rate to account for the modeled plant nutrient demand. This is often an underestimate of real world practices as discussed in the last paragraph of section 3.3. We are currently working on how to best address this discrepancy within the EPIC-CMAQ modeling system.

13. *L717: please explain the exact regions and locations.*

Specified the regions in Lines 719-722 as:

"Underestimates of soil N in some regions with an abundance of animal farms, such as parts of Colorado, New Mexico, north Texas, California, the Northeast U.S., and the Midwest, may be attributed to the lack of representation of farm-level manure N management practices, in which manure application can exceed the EPIC estimate of optimal crop demand."

14. *L752-753: it could be helpful to show the general performance on the dry and wet conditions used (simulated by other models).*

Fig. S7 in supplementary material shows estimated low soil moisture to also exhibit very dry conditions in Texas for May and July 2011, while relatively moist conditions with highest soil moisture in the Northeast and Pacific Northwest primarily in May 2011. Hence, the WRF meteorological model simulation for soil moisture for both dry and wet conditions in this paper performs reasonably well in comparison to the actual reported wet and dry conditions in 2011 as reported by NOAA’s Palmer indices for wet and dry conditions across CONUS in 2011, as cited in Line 753.

15. *L760: it may be good to indicate from literature the importance of manure management (e.g., compared to N fertilizer) in these regions.*

We do address the detrimental impact of land application as part of manure management in Lines 722-727:

“Farms in the vicinity of concentrated animal units often apply N in excess of the crop N requirements as part of the manure management strategy, typically increasing the N emissions (Montes et al., 2013). USDA has reported that confined animal units/livestock production correlates with increasing amounts of farm-level excess N (Kellogg et al., 2000; Ribaudo and Sneeringer, 2016). Model representations of these practices are needed to better estimate the impact of nitrogen in the environment.”

To clarify the importance of manure management compared to N fertilizer in the U.S., we present the further explanation in Lines 764-773:

“In the U.S., 60 percent of Nitrogen from manure produced on animal feedlot operations cannot be applied to their own land because they are in ‘excess’ of USDA advised agronomic rates. Most U.S. counties with animal farms have adequate crop acres not associated with animal operations, but within the county, on which it is feasible to spread the excess manure at agronomic rates at certain additional cost. However, 20 percent of the total U.S. on-farm excess manure nitrogen is produced in counties with insufficient cropland for its application at agronomic rates (Gollehon et al., 2001). For areas without adequate land, alternatives to local land application such as energy production (for example, biofuel) are needed. In absence of such a mitigation strategy, excess manure N applied on soil contributes is susceptible to reactive N emissions and leaching (Ribaudo et al., 2003; Ribaudo et al., 2012).”

The following citations are added in ‘reference’ section:

Gollehon, N. R., Caswell, M., Ribaudo, M., Kellogg, R. L., Lander, C., and Letson, D.: Confined animal production and manure nutrients, United States Department of Agriculture, Economic Research Service, 2001.

Ribaudo, M., Livingston, M., and Williamson, J.: Nitrogen management on us corn acres, 2001-10, United States Department of Agriculture, Economic Research Service, 2012.

Ribaudo, M., Gollehon, N., and Agapoff, J.: Land application of manure by animal feeding operations: Is more land needed?, Journal of Soil and Water Conservation, 58, 30-38, 2003.

16. *It is the first process-based scheme in a photochemical model. But authors may need to mention where this kind of mechanisms have been used before (e.g., crop models, terrestrial vegetation models, etc.), and the advantages.*

We already have addressed the advantages of using mechanistic model like DayCENT and listed similar process-based models in Lines 369-381:

“One of the advantages of using DayCENT is its ability to simulate all types of terrestrial ecosystems. DayCENT is one of the only biogeochemical models which not only provides a process-based representation of soil N emissions, but has also been calibrated and validated across an array of conditions for crop productivity, soil C, soil temperature and water content, N_2O, and soil NO_3^- (Necpálová et al., 2015). Hence, mechanistic models like DayCENT yield more reliable results by applying validated controls of soil properties like soil temperature and moisture, which are the key process controls to nitrification and denitrification. More recent mechanistic models like DNDC, MicNit, ECOSYS, and COUPMODEL are quite similar to DayCENT in their representation of nitrification and denitrification process. However, these models have not been as widely evaluated and impose greater computational costs (Butterbach-Bahl et al., 2013). DayCENT also enhances consistency in our mechanistic model by utilizing the same C-N mineralization scheme (taken from the CENTURY model (Parton et al., 2001)) that is used in EPIC.”

Minor remarks:

L346: Wang et al.: please provide the year of this publication.

Wang et al. (1998), edited in Line 347

L457: NH4+?

NH_4 changed to NH_4^+ in Line 458

Response to RC2: Anonymous Referee #2:

Comment 1: *Figure 3. The authors explain the results due to "likely" causes. Figure 3c does not convey clearly the results intended by the authors. This part should be clarified.*

To clarify, we referred to 'likely' causes in Lines 610-615 as the differences between BDSNP implemented in GEOS-Chem (Hudman et al., 2012) and in CMAQ (Rasool et al., 2016) to be the finer land use definition and daily scale and finer resolution EPIC soil N data, which has been illustrated in greater detail in Rasool et al. (2016). Fig. 3c on the other hand is the nitrogen oxide flux from the mechanistic scheme, which has a dynamic representation of C-N mineralization, absent in both YL and BDSNP. We further edited Lines 612-617 as:

"Hudman et al. (2012) found nearly twice as large of a gap between BDSNP and YL in GEOS-Chem; the narrower gap here likely results from our use of sub-grid biome classification and EPIC fertilizer data (Rasool et al., 2016). The mechanistic scheme (Figure 3c) generates emission estimates that are closer to the YL scheme but with greater spatial and temporal heterogeneity, reflecting its use of a more dynamic soil N and C pools."

Comment 2: *It also appears that the process-based methods introduced in the CMAQ framework cannot be rigorously tested due to lack or old data, which detracts somehow from the considerable efforts made to improve the accuracy in soil N emission predictions. Presentation quality is fine.*

This work highlights the scarcity and need of observation of soil nitrogen fluxes (especially NO_x, HONO and NH_3 that affect air quality) on a frequent basis and in more locations.

Firstly, agricultural study sites such as the Kellogg Biological Station (https://lter.kbs.msu.edu/datatables/177) are quite rare and not well aligned with ambient air quality observation networks. Secondly, the N_2O measured at agricultural sites is unaccounted for in most chemical transport models like CMAQ. In addition, these chamber studies are designed more with the aim of looking at difference between various management practices on a field scale, which would require running different simulations of biogeochemical models (EPIC or DAYCENT), which is computationally expensive for a regional scale (CONUS) implementation like this, but ideally extend to future research plans.

However, improvements in modeled estimates in comparison to observed OMI NO_2 column, measured concentrations of NO_x, O_3, $PM_{2.5}$ NO_3 and some available soil NO emission rates, with 'Mechanistic' scheme does provide an indication that we are moving towards the right direction.

Comment 3: *Whenever possible, authors should include estimates of estimation or observational errors (e.g. Table 3).*

Table 3 gives the comparison of maximum soil NO emission rates observed for various sites with those corresponding to the three modeling approaches presented ('YL', BDSNP' and 'Mech.').

Comment 4: *Abbreviations used in tables and figures should be explained in the table titles or figure captions. Tables and figures should stand on their own.*

Edits have been made to define abbreviations at first use in both tables and figures as well.

Comment 5: *Since CMAQ already uses EPIC to simulate NH3 bi-directional exchange, the authors should acknowledge recent documentation of process-based denitrification approaches used in EPIC: Izaurralde et al. (2017). Ecol. Modelling 359:349-362 doi:10.1016/j.ecolmodel.2017.06.007. (see line 481).*

Izaurralde et al. (2017) added to line 482, with full citation in ‘reference’ section as:

Izaurralde, R. C., McGill, W. B., Williams, J. R., Jones, C. D., Link, R. P., Manowitz, D. H., Schwab, D. E., Zhang, X., Robertson, G. P., and Millar, N.: Simulating microbial denitrification with EPIC: Model description and evaluation, Ecological modelling, 359, 349-362, 2017.

Comment 6: *The methodology and Figure 2 do not describe well the treatment of soil layer processes. EPIC simulates soil C and N transformation layer by layer up to 15. Is it the same for DayCent? How are the results from one model past to the other? Are these calculations done for the surface layer?*

EPIC is coupled with CMAQ through the FEST-C interphase to be compatible with the regional scale (CONUS) implementation in CMAQ. All EPIC output variables provided to CMAQ as input for calculating soil N emissions are for the soil depth from 0 to 1 cm and from 1 cm to 10 cm (prefixed as L1 and L2 in FEST-C), respectively. Bash et al. (2013) also modeled Ammonia evasion from soil and NH_4^+ nitrification losses for CMAQ, utilizing FEST-C interphase soil layers with depths of 1 cm and 10 cm, keeping things consistent in treatment of soil layers when it comes to treatment of different soil N cycling processes.

To clarify more, DAYCENT’s soil N gas sub-module was not run separately, but was ported and coded in the new ‘Mech.’ scheme in CMAQ and calculations in terms of soil layers were always consistent with the above-described approach for EPIC-CMAQ (i.e. top 10 cm soil layer, where the soil N cycling mostly occurs).

Briefly, the CONUS regional-scale implementation of EPIC and DAYCENT in CMAQ do not use all the soil layers except for topsoil (top 10 cm) used in the original plot-scale implementations of EPIC and DAYCENT. This is justified, as total N-cycling microbial biomass (N and C) in topsoil are about one to two orders of magnitude higher than that in subsoils (> 10 cm). This suggests that N cycling mainly occurred in topsoil, given that exponential declines in soil C and N resources occur in subsoils (Tang et al., 2018). Non-agricultural soil nutrient and properties data used in the new ‘Mechanistic’ scheme were available for the top 30 cm soil layer from the most recent global compilation of such data across different biomes (Xu et al., 2015), but are still consistent with the topsoil (i.e., top 10 cm L1 + L2) configuration for N cycling as used in this work. This is supported by the fact that studies have shown topsoil depth (even 0-5 cm) mineralizable N to be representative of the 0–30 cm depth, as 0-15 cm N-cycling biomass drops considerably as it reaches 10 cm depth and is significantly higher than N-cycling biomass available at soil depths > 15 cm (Dessureault-Rompré et al., 2016).

Dessureault-Rompré, J., Zebarth, B.J., Burton, D.L. and Grant, C.A.: Depth distribution of mineralizable nitrogen pools in contrasting soils in a semi-arid climate. *Canadian Journal of Soil Science*, *96*(1), pp.1-11, 2016.

Tang, Y., Yu, G., Zhang, X., Wang, Q., Ge, J., & Liu, S.: Changes in nitrogen-cycling microbial communities with depth in temperate and subtropical forest soils. *Applied Soil Ecology*, *124*, 218-228, 2018.

Xu et al. (2015) is in ‘reference’ section in main manuscript

Comment 7: *The authors should mention what impact could have an increase in the spatial resolution of the simulation in order to better capture the soil / management heterogeneity.*

Spatial scale-dependent variation in soil/management heterogeneity can substantially influence how an analysis has to be approached; i.e. whether to opt for regional scale or more of plot-scale (<10m). Implications of various spatial resolution in soil ecology are manifold one of which is pertaining to microbial-plant community diversity. However, how heterogeneity in soil bacterial communities influences biogeochemical soil N cycling between local (< 10 m) and landscape (e.g., CONUS 12 km x 12 km in our case) scales still needs further research (O'Brien et al., 2016).

O'brien, S.L., Gibbons, S.M., Owens, S.M., Hampton-Marcell, J., Johnston, E.R., Jastrow, J.D., Gilbert, J.A., Meyer, F. and Antonopoulos, D.A.: Spatial scale drives patterns in soil bacterial diversity. *Environmental microbiology*, *18*(6), pp.2039-2051, 2016.

Mechanistic representation of soil nitrogen emissions in the Community Multi-scale Air Quality (CMAQ) model v 5.1

Quazi Z. Rasool[1*], Jesse O. Bash[2] and Daniel S. Cohan[1]

[1]{Department of Civil and Environmental Engineering, Rice University, Houston, Texas, USA}

[2]{Computational Exposure Division, National Exposure Research Laboratory, Office of Research and Development, US Environmental Protection Agency, RTP, NC, USA}

*Currently at Department of Environmental Science and Engineering, UNC- Chapel Hill, NC, USA

Correspondence to: Quazi Rasool (qzr1@email.unc.edu)

Abstract

Soils are important sources of emissions of nitrogen (N)-containing gases such as nitric oxide (NO), nitrous acid (HONO), nitrous oxide (N_2O), and ammonia (NH_3). However, most contemporary air quality models lack a mechanistic representation of the biogeochemical processes that form these gases. They typically use heavily parameterized equations to simulate emissions of NO independently from NH_3, and do not quantify emissions of HONO or N_2O. This study introduces a mechanistic, process-oriented representation of soil emissions of N species (NO, HONO, N_2O, and NH_3) that we have recently implemented in the Community Multi-scale Air Quality (CMAQ) model. The mechanistic scheme accounts for biogeochemical processes for soil N transformations such as mineralization, volatilization, nitrification, and denitrification. The rates of these processes are influenced by soil parameters, meteorology, land use, and mineral N availability. We account for spatial heterogeneity in soil conditions and biome types by using a global dataset for soil carbon (C) and N across terrestrial ecosystems to estimate daily mineral N availability in non-agricultural soils, which was not accounted in earlier parameterizations for soil NO. Our mechanistic scheme also uses daily year-specific fertilizer use estimates from the Environmental Policy Integrated Climate (EPIC v.0509) agricultural model. A soil map with sub-grid biome definitions was used to represent conditions over the continental United States. CMAQ modeling for May and July 2011 shows improvement in model performance in simulated NO_2 columns compared to Ozone Monitoring Instrument (OMI) satellite retrievals for regions where soils are the dominant source of NO emissions. We also assess how the new scheme affects model performance for NO_x ($NO+NO_2$), fine nitrate (NO_3) particulate matter, and ozone observed by various ground-based monitoring networks. Soil NO emissions in the new mechanistic scheme tend to fall between the magnitudes of the previous parametric schemes and display much more spatial heterogeneity. The new mechanistic scheme also accounts for soil HONO, which had been ignored by parametric schemes.

1 Introduction

Global food production and fertilizer use are projected to double in this half-century in order to meet the demand from growing populations (Frink et al., 1999; Tilman et al., 2001). Increasing nitrogen (N) fertilization to meet food demand has been accompanied by increasing soil N emissions across the globe, including in the United States (Davidson et al., 2011). N fertilizer consumption globally has increased from 0.9 to 7.4 g N per m^{-2} cropland yr^{-1} between 1961-2013, with the U.S. still among the top five N fertilizer users in the world (Lu and Tian, 2017). U.S. N fertilizer use increased from 0.28 to 9.54 g N m^{-2} yr^{-1} during 1940 to 2015. In the past century, hotspots of N fertilizer use have shifted from the southeastern and eastern U.S. to the Midwest and the Great Plains comprising the Corn Belt region (Cao et al., 2017). Recent studies have pointed to soils as a significant source of NO_x emissions, contributing ~ 20% to the total budget globally and larger fractions over heavily fertilized agricultural regions (Jaeglé et al., 2005; Vinken et al., 2014; Wang et al., 2017). ~~Soil NO emissions tend to peak in the summertime, when they can contribute from 15-40% of total tropospheric NO_2 column in the continental U.S. (CONUS) (Williams et al., 1992; Hudman et al., 2012; Rasool et al., 2016). Summer is also the peak season for ozone concentrations (Cooper et al., 2014; Strode et al., 2015) and the time when photochemistry is most sensitive to NO_x (Simon et al., 2014).~~

Formatted: Font: Italic

Despite the significance of NO_x emissions generated by soil microbes, policies both globally and for CONUS have focused largely on limiting mobile and point fossil fuel sources of NO_x (Li et al., 2016). Hence, it is incumbent to strategize for reduction of non-point soil sources of NO_x emissions, especially in agricultural areas. Recent studies have shown higher soil NO_x even in non-agricultural areas like forests to significantly impact summertime ozone in CONUS (Hickman et al., 2010; Travis et al., 2016). Consequently, it is increasingly important to estimate both N fertilizer-induced and non-agricultural NH_3 and NO_x emissions in air quality models.

Soil NO emissions tend to peak in the summertime, when they can contribute from 15-40% of total tropospheric NO_2 column in the continental U.S. (CONUS) (Williams et al., 1992; Hudman et al., 2012; Rasool et al., 2016). Summer is also the peak season for ozone concentrations (Cooper et al., 2014; Strode et al., 2015) and the time when photochemistry is most sensitive to NO_x (Simon et al., 2014). N oxides (NO_x = NO + NO_2) worsen air quality and threaten human health directly and by contributing to the formation of other pollutants. NO_x drives the formation of tropospheric ozone and contributes to a significant fraction of both inorganic and organic particulate matter (PM) (Seinfeld and Pandis, 2012; Wang et al., 2013). Global emissions of NO_x are responsible for one in eight premature deaths worldwide as reported by the World Health Organization (Neira et al., 2014). The premature deaths are a result of the link of these pollutants to cardiovascular and chronically obstructive pulmonary (COPD) diseases, asthma, cancer, birth defects, and sudden infant death syndrome. These adverse health impacts have been shown to worsen with the rising rate of reactive N emissions from soil N cycling (Kampa and Castanas, 2008; Townsend et al., 2003). NO_x indirectly impacts Earth's radiative balance by modulating concentrations of OH radicals, the dominant oxidant of certain greenhouse gases such as methane (IPCC, ~~2007~~2013; Steinkamp and Lawrence, 2011). Nitrous acid (HONO) upon photolysis releases OH radicals along with NO, driving tropospheric ozone and secondary aerosol formation (Pusede et al., 2015). Soils and agriculture are the leading emitters of N_2O~~, emissions from soils primarily through agriculture significantly contribute to warming of global average temperature on the longer 20 and 100 years timescales, more than both CO_2 and CH_4~~ a potent greenhouse gas (~~Pinder et al., 2012~~IPCC, 2013).

Ammonia (NH_3) also contributes to a large fraction of airborne fine particulate matter ($PM_{2.5}$) (Kwok et al., 2013). Elevated levels of $PM_{2.5}$ are linked to various adverse cardiovascular ailments such as irregular heartbeat and aggravated asthma that cause premature death (Pope et al., 2009), and contribute to visibility impairment through haze (Wang et al., 2012). NH_3 gaseous emissions also influence the nucleation of new particles (Holmes, 2007). Air quality models such as, Community Multiscale Air Quality (CMAQ) model and GEOS-Chem represent the bidirectional NH_3 exchange between the atmosphere and soil-vegetation, analyzed under varied soil, vegetative, and environmental conditions (Cooter et al., 2012; Bash et al., 2013; Zhu et al. 2015).

NO_x, NH_3, HONO, and N_2O are produced from both microbial and physicochemical processes in soil N cycling, predominantly nitrification and denitrification (Medinets et al., 2015; Parton et al., 2001; Pilegaard, 2013; Su et al., 2011). Nitrification is oxidation of NH_4^+ to NO_3^- where intermediate species such as NO and HONO are emitted along with relatively small amounts of N_2O as byproducts. Denitrification is reduction of soil NO_3^-; it produces some NO, but predominantly produces N_2O and N_2 (Firestone and Davidson, 1989; Gödde and Conrad, 2000; Laville et al., 2011; Medinets et al., 2015). The fraction of N emitted as NO and HONO relative to N_2O throughout nitrification and denitrification depends on several factors: soil temperature; water filled pore space (WFPS), which in turn depends on soil texture and soil water content; gas diffusivity; and soil pH. HONO is produced during nitrification only and is a source of NO and OH after undergoing photolysis (Butterbach-Bahl et al., 2013; Conrad, 2002; Ludwig et al., 2001; Oswald et al., 2013; Parton et al., 2001; Venterea and Rolston, 2000).

Whether N_2O or N_2 become dominant during denitrification depends on the availability of soil NO_3^- relative to available carbon (C), WFPS, soil gas diffusivity, and bulk density (i.e., dry weight of soil divided by its volume, indicating soil compaction/aeration by O_2). Denitrification rates are quite low even at high soil N concentrations if available soil C is absent. However, the presence of high NO_3 concentrations with sufficient available C is the inhibiting factor for conversion of N_2O to N_2, keeping N_2O emissions dominant during denitrification (Weier et al., 1993; Del Grosso et al., 2000). Denitrification N_2O emissions are also found to increase with a decrease in soil pH in the range of 4.0 to 8.0 generally (Liu et al., 2010). Fertilizer application and wet and dry deposition add to the soil NH_4 and NO_3 pools, which undergo transformation to emit soil N as intermediates of nitrification and denitrification (Kesik et al., 2006; Liu et al., 2006; Redding et al., 2016; Schindlbacher et al., 2004).

Soil moisture content is the strongest determinant of nitrification and denitrification rates and the relative proportions of various N gases emitted by each. Increasing soil water content due to wetting events such as irrigation and rainfall can stimulate nitrification and denitrification. Nitrification rates peak 2-3 days after wetting, when excess water has drained away and the rate of downward water movement has decreased. Denitrification rates substantially increase and nitrification rates become much slower in wetter soils. This is also influenced by soil texture; for instance, denitrification is favored in poorly drained clay soils and nitrification is favored in freely draining sandy soils (Barton et al., 1999; Parton et al., 2001).

WFPS is a metric that incorporates the above factors. Relative proportions of NO, HONO, and N_2O emitted vary with WFPS. Dry aerobic conditions (WFPS ~ 0-55%) are optimal for nitrification, with soil NO dominating soil N gas emissions at WFPS ~ 30–55% (Davidson and Verchot, 2000; Parton et al., 2001). HONO emissions have been observed up to WFPS of 40% and dominate N gas emissions under very dry and acidic soil conditions (Maljanen et al., 2013; Mamtimin et al., 2016; Oswald et al., 2013; Su et al, 2011). Nitrification influences N_2O

production within the range of 30–70% WFPS, whereas denitrification dominates N_2O production in wetter soils. Denitrification N_2O is limited by lower WFPS in spite of sufficient available NO_3^- and C (Butterbach-Bahl et al., 2013; Del Grosso et al., 2000; Hu et al., 2015; Medinets et al., 2015; Weier et al., 1993). As a result, NO and HONO emissions tend to decrease with increasing water content, whereas N_2O emissions increase subject to available NO_3^- and C (Parton et al., 2001; Oswald et al., 2013).

Extended dry periods also suppress soil NO emissions, by limiting substrate diffusion while water-stressed nitrifying bacteria remain dormant, allowing N substrate (NH_4^+ or organic N) to accumulate (Davidson, 1992; Jaeglé et al., 2004; Hudman et al., 2010; Scholes et al., 1997). Re-wetting of soil by rain reactivates these microbes, enabling them to metabolize accumulated N substrate (Homyak et al., 2016). The resulting NO pulses can be 10–100 times background emission rates and typically last for 1–2 days (Yienger and Levy, 1995; Hudman et al., 2012; Leitner et al., 2017).

Higher soil temperature is critical in increasing NO emission during nitrification under dry conditions. However, N_2O generated in denitrification positively correlates with soil temperature only when WFPS and N substrate availability in soil are not the limiting factors (Machefert et al., 2002; Robertson and Groffman, 2007). Recently, a nearly 38% increase in NO emitted was observed under dry conditions (~ 25-35 % WFPS) in California agricultural soils when soil temperatures rose from 30-35 to 35-40 °C (Oikawa et al., 2015). Temperature-dependent soil NO_x emissions may strongly contribute to the sensitivity of ozone to rising temperatures (Romer et al., 2018). Also, some soil NO is converted to NO_2 and deposited to the plant canopy, reducing the amount of NO_x entering the atmosphere (Ludwig et al., 2001).

Mechanistic models of soil N emissions already exist and are used in the earth science and soil biogeochemical modeling community (Del Grosso et al., 2000; Manzoni and Porporato, 2009; Parton et al., 2001). However, photochemical models like CMAQ have been using a mechanistic approach only for NH_3, while using simpler parametric approaches for NO (Bash et al., 2013; Rasool et al., 2016). Other N oxide emissions like HONO and N_2O are absent from the parametric schemes used in CMAQ (Butterbach-Bahl et al., 2013; Heil et al., 2016; Su et al., 2011). Variability in soil physicochemical properties like pH, temperature, and moisture along with nutrient availability strongly control the spatial and temporal trends of soil N compounds (Medinets et al., 2015; Pilegaard, 2013).

EPA's Air Pollutant Emissions Trends Data shows anthropogenic sources of NO_x (excluding fertilizers) fell by 60 percent in the U.S. since 1980, heightening the relative importance of soils. Area sources of NO_x like soils along with less than expected reduction in off-road anthropogenic sources are believed to have contributed to a slowdown in US NO_x reductions from 2011-2016 (Jiang et al., 2018). Hence, accurate and consistent representation of soil N is needed to address uncertainties in their estimates.

Parameterized schemes currently implemented in CMAQ for CONUS like Yienger-Levy (YL) and the Berkeley Dalhousie Soil NO Parameterization (BDSNP) consider only NO expressed as a fraction of total soil N available, without differentiating the fraction of soil N that occurs as organic N, NH_4, or NO_3 (Hudman et al., 2012; Rasool et al., 2016; Yienger and Levy, 1995). Moreover, these parametric schemes classify soil NO emissions as constant factors for different non-agricultural biomes/ecosystems, compiled from reported literature and field estimates worldwide (Davidson and Kingerlee, 1997; Steinkamp and Lawrence, 2011; Yienger and Levy, 1995). These emission factors account for the baseline biogenic NO_x emissions in addition to sources from deposition (all biomes) and fertilizer (agricultural land-cover only) in the latest BDSNP parameterization (Hudman et al., 2012; Rasool et al., 2016). Despite their limitations, parameterized schemes do distinguish which biomes exhibit low NO emissions (wetlands, tundra, and temperate or boreal forests) from those producing high soil NO (grasslands, tropical savannah or woodland and agricultural fields) (Kottek et al., 2006; Rasool et al., 2016; Steinkamp and Lawrence, 2011).

The U.S. Environmental Protection Agency (EPA) recently coupled CMAQ with U.S. Department of Agriculture's (USDA) Environmental Policy Integrated Climate (EPIC) agro-ecosystem model. This integrated EPIC-CMAQ framework accounts for a process-based approach for NH_3 by modeling its bidirectional exchange (Nemitz et al., 2001; Cooter et al., 2010; Pleim et al., 2013). The coupled model uses EPIC to simulate fertilizer application rate, timing, and composition. Then, CMAQ estimates the spatial and temporal trends of the soil ammonium (NH_4^+) pool by tracking the ammonium mass balance throughout processes like fertilization, volatilization, deposition, and nitrification (Bash et al., 2013). Using the EPIC-derived soil N pool better represents the seasonal dynamics of fertilizer-induced N emissions across CONUS (Cooter et al., 2012). The coupling with EPIC reduces CMAQ's error and bias in simulating total NH_3 + NH_4^+ wet deposition flux and ammonium related aerosol concentrations (Bash et al., 2013). BDSNP parametric scheme implemented in CMAQ also uses the daily soil N pool from EPIC (Rasool et al., 2016).

Our work builds a new mechanistic approach for modeling soil N emissions in CMAQ based on DayCENT (Daily version of CENTURY model) biogeochemical scheme (Del Grosso et al., 2001; Parton et al., 2001), integrating nitrification and denitrification mechanistic processes that generate NO, HONO, N_2O, and N_2 under different soil conditions and meteorology. We compare the NO and HONO emissions estimates and associated estimates of tropospheric NO_2 column, ozone, and $PM_{2.5}$ with those obtained from CMAQ using the YL and BDSNP parametric schemes. For agricultural biomes, our mechanistic scheme uses daily soil N pools from the same EPIC simulations as in Rasool et al. (2016). Unlike BDSNP, which uses a total weighted soil N, the new mechanistic model tracks different forms of soil N as NH_4, NO_3, and organic N for different soil layers and vegetation types so that, nitrification and denitrification can be represented. For non-agricultural biomes, our new mechanistic scheme uses a global soil nutrient dataset in an updated C and N mineralization framework. This enables the model to track the conversion of organic soil N to NH_4 and NO_3 pools on a daily scale for non-agricultural soils.

2 Methodology

2.1 Overview of soil N schemes

Key features of the YL and BDSNP parametric soil NO schemes and our new mechanistic scheme for soil NO, HONO, and N_2O are illustrated in Figure 1 and Table 1.

The YL scheme, based on Yienger and Levy (1995), parameterizes soil NO emission ($S_{NO_{YL}}, in\ ng-N\ m^{-2}\ s^{-1}$) in Equation 1 as a function of biome specific emissions factor (A_{biome}) and soil temperature (T_{soil}).

$$S_{NO_{YL}} = f_{\frac{w}{d}}\left(A_{biome(w/d)}, T_{soil}\right) P(precipitation) CRF(LAI, SAI) \qquad (1)$$

The emissions factor depends on whether the soil is wet ($A_{biome(w)}$) or dry ($A_{biome(d)}$), with the wet factor used when rainfall exceeds one cm in the prior two weeks. For dry soils, YL assumes NO emissions exhibit a small and linear response to increasing soil temperatures. For wet soils, soil NO is zero for frozen conditions, increases linearly from 0 to 10°C, and increases exponentially from 10 to 30°C, after which it is constant. In agricultural regions, YL assumes wet conditions throughout the growing season (May – September) and assumes 2.5% of the fertilizer applied N is emitted as NO, in addition to a baseline NO emissions rate based on grasslands. The pulsing term (*P*(*precipitation*)) is applied if precipitation follows at least two dry weeks. The canopy reduction factor (*CRF*) is set as a function of leaf area index (*LAI*) and stomatal area index (*SAI*).

Biogenic Emissions Inventory System (BEIS v.3.61 used in current versions of CMAQ (v5.0.2 or higher) estimates NO emissions from soils essentially using the same original YL algorithm as in Equation 1, with slight updates accounting for soil moisture, crop canopy coverage, and fertilizer application. The YL soil NO algorithm in CMAQ distinguishes between agricultural and nonagricultural land use types (Pouliot and Pierce, 2009). Adjustments due to temperature, precipitation (pulsing), fertilizer application, and canopy uptake are limited to the growing season, assumed as April 1 to October 31, and are restricted to agricultural areas as defined by the Biogenic Emissions Landuse Database (BELD). Unlike the original YL, the implementation of YL in CMAQ (CMAQ-YL) interpolates between wet and dry conditions based on soil moisture in the top layer (1cm). In this study, we use the Pleim-Xiu Land Surface Model (PX-LSM) in CMAQ to compute soil temperature (T_{soil}) and soil moisture (θ_{soil}).

Agricultural soil NO emissions are based on the baseline grassland NO emission ($A_{grassland}$) plus an additional factor ($Fertilizer(t)$) that starts at its peak value during the first month of the growing season and declines linearly to zero at the end of the growing season. The growing season is defined as April-October in CMAQ-YL, rather than being allowed to vary by latitude (original YL) or by a satellite driven analysis of vegetation (original BDSNP). A summary of the modified YL algorithm is presented below for growing season agricultural emissions (Equation 2).

$$S_{NO_{CMAQ-YL},\ Agricultural\ growing\ season} =$$

$$f\left(A_{grassland} + Fertilizer(t), T_{soil}, \theta_{soil}\right)P(precipitation)CRF(LAI, SAI) \qquad (2)$$

For non-growing season or non-agricultural areas throughout the year, soil NO emissions are assumed to depend only on temperature and the base emissions for different biomes (A_{biome}) as provided in BEIS. CMAQ still uses the base emission for both agricultural and non-agricultural land types with adjustments based solely on air temperature ($T_{air,in\ K}$) as done in BEIS (Equation 3). However, for sake of simplicity we refer to 'CMAQ-YL' merely as 'YL' ~~only in figures, conclusion, result and discussions, hereon~~.

$$S_{NO_{CMAQ-YL},\ non-agricultural\ or\ non-growing\ season}$$
$$= (A_{biome})e^{(0.04686 * T_{air} - 14.30579)} \qquad (3)$$

The original implementation of the BDSNP scheme in CMAQ v5.0.2 was described by Rasool et al. (2016). Here, we update that code for CMAQv5.1, but the formulation remains the same. Soil NO emissions, S_{NO}, are computed in Equation 4 as the product of biome specific emission rates ($A_{biome}(N_{avail})$) and adjustment factors to represent the influence of ambient conditions. The biome specific emission rates have background soil NO for 24 MODIS biome types from literature (Stehfest and Bouwman, 2006; Steinkamp and Lawrence, 2011). Fertilizer and deposition emission rates based on an exponential decay after input of fertilizer and deposition N are added to background soil NO emission rates for respective biomes. BDSNP accounts for total N from fertilizer and deposition obtained from EPIC. EPIC provides the N available from crop-specific fertilizer soil N pool in different forms as: NH_4, NO_3, and organic N. A final weighted total soil N pool is used by weighting the different N forms by the fraction of each crop type in each modeling grid. The soil temperature response $f(T_{soil})$ is an exponential function of temperature (in K). Unlike YL that depends solely on rainfall, BDSNP has a Poisson function $g(\theta)$ based on soil moisture (θ) that increases smoothly first until a maximum and then decreases when soil becomes water-saturated. BDSNP also differentiates between wet and dry soil conditions and provides more detailed representation than YL of pulsing following precipitation and of the CRF (described in section 2.5).

$$S_{NO_{BDSNP}} = A_{biome}(N_{avail})\, f(T) g(\theta) P\left(l_{dry}\right) CRF(LAI, Meterology, Biome) \qquad (4)$$

Our new mechanistic scheme computes soil emissions of NO, HONO, and N_2O by specifically representing both nitrification and denitrification. Equations 5-7 provide an overview of the mechanistic formulation. All functions are described in greater detail in Section 2.6.4. In the equations, the pulsing factor $P\left(l_{dry}\right)$ follows the formulation of Rasool et al. (2016). The canopy reduction factor $CRF(LAI, Meteorology, Biome)$ is described in section 2.5. Briefly, we note that nitrification rates ($R_N\ in\ Eq. 24,\ kg-N/ha\ per\ s$) depend on the available NH_4 pool, soil temperature (T_{soil}), soil moisture (θ_{soil}), gas diffusivity (Dr), and pH adjustment factors. Meanwhile, denitrification rates ($R_D\ in\ Eq. 25,\ kg-N/ha\ per\ s$) depend on available NO_3 pool, relative availability of NO_3 to C, soil temperature, gas diffusivity, and soil moisture adjustment factors.

$$S_{NO} = \begin{pmatrix} N_{NO_x} - S_{HONO} \\ + \\ D_{NO} \end{pmatrix} CRF(LAI, Meteorology, Biome)$$

$$\equiv \begin{pmatrix} f(NH_4, T_{soil}, \theta_{soil}, Dr, pH) P\left(l_{dry}\right) \\ + \\ f(NO_3{:}C, T_{soil}, \theta_{soil}, Dr) \end{pmatrix} CRF(LAI, Meteorology, Biome) \qquad (5)$$

$$S_{HONO} = (HONO_f)(N_{NO_x})(f_{SWC}) CRF(LAI, Meteorology, Biome)$$

$$\equiv (HONO_f)\left(f(NH_4, T_{soil}, \theta_{soil}, Dr, pH) P\left(l_{dry}\right)\right)(f_{SWC}) CRF(LAI, Meteorology, Biome) \qquad (6)$$

$$S_{N_2O} = \begin{pmatrix} N_{N_2O} \\ + \\ D_{N_2O} \end{pmatrix} \equiv \begin{pmatrix} f(NH_4, T_{soil}, \theta_{soil}, Dr, pH) \\ + \\ f(NO_3{:}C, T_{soil}, \theta_{soil}, Dr) \end{pmatrix} \qquad (7)$$

In all our simulations, soil NH_3 emission is calculated based on the bi-directional exchange scheme (Bash et al., 2013) in CMAQ.

2.2 Biome classification over CONUS

CMAQ uses the National Land Cover Database with 40 classifications (NLCD40, https://www.mrlc.gov/) to represent land cover, which is used by the YL parametric scheme. However, Steinkamp and Lawrence (2011) provide soil NO emission factors ($A'_{biome}(N_{avail})$) for only 24 MODIS biomes in the BDSNP parametric scheme. Thus, the initial implementation of BDSNP in CMAQ by Rasool et al. (2016) introduced a mapping between MODIS 24 and NLCD40 biomes to set an emission factor for each NLCD40 biome type (see Appendix Table A2). Factors were then adjusted using Köppen climate zone classifications (Kottek et al., 2006). Whereas the original implementation of BDSNP by Rasool et al. (2016) treated each grid cell based on its most prevalent biome type, our update of BDSNP for CMAQv5.1 and our mechanistic model use sub-grid biome classification, accounting for the fraction of each biome type in each cell.

The latest Biogenic Emissions Landcover Database version 4 (BELD4), generated using the BELD4 tool in the SA Raster Tools system, is used to represent land cover types consistently across both the Fertilizer Emission Scenario Tool for CMAQ (FEST-C v1.2, https://www.cmascenter.org/fest-c/); and the Weather Research and Forecast (WRF) meteorological model (Skamarock et al., 2008)/CMAQ framework. BEIS v3.61 within CMAQ integrates BELD4 with other data sources generated at 1-km resolution to provide fractional crop and vegetation cover. U.S. land use categories are based on the 2011 NLCD40 categories. FEST-C provides tree and crop percentage coverage for 194 tree classes and 42 crops (https://www.cmascenter.org/sa-tools/documentation/4.2/Raster_Users_Guide_4_2.pdf). For determining fractional crop cover, the 2011 NLCD/MODIS data was used for Canada and the U.S. in BELD4 data generation tool of FEST-C. Tree species fractional coverage is based on 2011 Forest Inventory and Analysis (FIA) version 5.1. MODIS satellite products are used where detailed data is unavailable outside of the U.S.

2.3 N Fertilizer

The YL scheme set fertilizer-driven soil NO emissions to be proportional to fertilizer application during a prescribed growing season: May-August for the Northern Hemisphere and November-

February for the Southern Hemisphere (Yienger and Levy, 1995) or April-October for CMAQ-YL. Our implementations of both BDSNP parameterization and mechanistic soil N schemes into CMAQ are designed to enable the use of year- and location-specific fertilizer data with daily resolution. We use FEST-C to incorporate EPIC fertilizer application data into our CMAQ runs. EPIC estimates daily fertilizer application based entirely on simulated idealized plant demand with N stress and limitations in response to local soil and weather conditions, using linkages with WRF via FEST-C. The FEST-C interface also ensures EPIC simulations are spatially consistent with CMAQ's CONUS domain and resolution through the Spatial Allocator (SA) Raster Tools system (http://www.cmascenter.org/sa-tools/).

Because EPIC covers only the U.S., outside the U.S. BDSNP use fertilizer data regridded from Hudman et al. (2012), which scaled Potter et al. (2010) data for fertilizer N from 1994-2001 to global fertilizer levels in 2006. Our mechanistic scheme uses a more recently compiled and speciated soil N and C dataset for non-U.S. agricultural regions, regridded from Xu et al. (2015).

2.4 N Deposition

N deposition serves as a significant addition to the soil mineral N (inorganic N: NH_4^+ and NO_3^-) pool and hence influences soil N emissions. The YL scheme does not explicitly represent N deposition but instead sets soil emissions based on biome type. In our implementation of both updated BDSNP and new mechanistic soil N schemes, hourly wet and dry deposition rates for both reduced and oxidized forms of N, computed within the CMAQ simulation, are added to the NH_4^+ and NO_3^- soil pools.

2.5 Canopy reduction factor (CRF)

CRF is used to calculate above canopy NO and HONO, assuming that some fraction of each is converted to NO_2 and absorbed by leaves. Earlier global scale GEOS-Chem simulations with BDSNP had a monthly averaged CRF that reduced total soil NO_x by an average of 16% (Hudman et al., 2012).

The original YL soil NO scheme (Yienger and Levy, 1995) and the in-line BEIS in CMAQ set CRF as a function of LAI and SAI. Recently, implementations of BDSNP in CMAQ and GEOS-Chem implemented CRF as a function of wind speed, turbulence, and canopy structure (Geddes et al., 2016; Rasool et al., 2016; Wang et al., 1998).

Here, we compute CRF using equations from Wang et al. (1998) for both BDSNP and the new mechanistic scheme using spatially and temporally variable land-surface parameters: surface (2 m) temperature, solar radiation (W/m^2), surface pressure, snow cover, wind speed (v_{wind}), cloud fraction, canopy structure, vegetation coverage (LAI and canopy resistances), gas diffusivity, and deposition coefficients. The final reduction factor ($CRF(LAI, Meteorology, Biome)$) for primary biogenic soil NO emissions is based on two main factors: bulk stomatal resistance (R_{Bulk}), and land-use specific ventilation velocity of NO ($v_{vent,NO}$), calculated based on the parameters mentioned above (Equation 8).

$$CRF(LAI, Meteorology, Biome) = \frac{R_{Bulk}}{R_{Bulk} + v_{vent,NO}} \quad (8)$$

Ventilation velocity of NO ($v_{vent,NO}$) is calculated by adjusting a normalized day and night specific velocity from Wang et al. (1998): 10^{-2} and 0.2×10^{-2} m/s, respectively. The adjustments are based on biome-specific LAI and canopy wind extinction coefficients (C_{Biome}). $C_{tropical\ rainforest}$ is the canopy wind extinction coefficient for tropical rain forests, the biome on which most canopy uptake studies for NO_x are based (Equation 9).

$$v_{vent,NO} = v_{vent,NO_{day/night}} \sqrt{\left(\frac{v_{wind}}{3}\right)^2 \left(\frac{7}{LAI}\right)} \left(\frac{C_{tropical\ rainforest}}{C_{Biome}}\right) \quad (9)$$

R_{Bulk} is a combination of various canopy resistances in series and parallel: internal stomatal resistance, cuticle resistance, and aerodynamic resistance which have biome specific normalized values for the MODIS 24 biomes also available in the dry deposition scheme of CMAQ. These normalized values of individual resistances are subsequently adjusted and dependent on multiple conditions for solar radiation, surface temperature, pressure, deposition coefficients and molecular diffusivity of NO_2 in air. The calculation of R_{Bulk} based on Wang et al. (1998) has been documented and shared in the open source BDSNP code repository (canopy_nox_mod.F) for the purpose of reproducibility, available at https://daac.ornl.gov/cgi-bin/dsviewer.pl?ds_id=1351.

2.6 Detailed description of the mechanistic soil N scheme

2.6.1 Overview

Our new mechanistic soil N model tracks the NH_4, NO_3, and organic C and N pools in soil separately, in contrast to the total N pool of BDSNP, and estimates NO, HONO, and N_2O rather than just NO (Figure 2). It uses DayCENT to represent both nitrification and denitrifiction. For agricultural biomes, we use speciated N and C pools from EPIC to drive DayCENT. For non-agricultural biomes, we use a C-N mineralization framework (Manzoni and Porporato, 2009) to estimate the inorganic N and C pools for DayCENT.

One of the advantages of using DayCENT is its ability to simulate all types of terrestrial ecosystems. DayCENT is one of the only biogeochemical models which not only provides a process-based representation of soil N emissions, but has also been calibrated and validated across an array of conditions for crop productivity, soil C, soil temperature and water content, N_2O, and soil NO_3^- (Necpálová et al., 2015). Hence, mechanistic models like DayCENT yield more reliable results by applying validated controls of soil properties like soil temperature and moisture, which are the key process controls to nitrification and denitrification. More recent mechanistic models like DNDC, MicNit, ECOSYS, and COUPMODEL are quite similar to DayCENT in their representation of nitrification and denitrification process. However, these models have not been as widely evaluated and impose greater computational costs (Butterbach-Bahl et al., 2013). DayCENT also enhances consistency in our mechanistic model by utilizing the same C-N mineralization scheme (taken from the CENTURY model (Parton et al., 2001)) that is used in EPIC.

Most stand-alone applications of DayCENT and other mechanistic models have focused on the biogeochemical, climate, and agricultural impacts of soil emissions. Our linkage of DayCENT with CMAQ provides an opportunity to for the first time estimate emissions of multiple soil N species through a process-based approach and then assess their impact on atmospheric chemistry in a regional photochemical model.

2.6.2 Agricultural regions

In agricultural regions, we use EPIC to derive organic N, NH_4, NO_3, and C pools updated on a daily scale. EPIC follows the same approach used in the CENTURY model (Parton et al., 1994), but uses an updated crop growth model, and better represents effect of sorption on soil water content that affect leaching losses and surface to sub-surface flow of N. In contrast, CENTURY used monthly water leached below 30-cm soil depth, annual precipitation, and the silt and clay content of soil (Izaurralde et al., 2006).

In EPIC, organic N residues added to the agricultural soil surface or belowground from plant/crop residues, roots, fertilizer, deposition and manure are split into two broad compartments: microbial or active biomass, and slow or passive humus. Slow or passive humus is essentially recalcitrant and non-living in nature with very slow turnover rates ranging from centuries to even thousands of years and makes up most of the organic matter. N uptake by soil microbes from organic matter, also called 'microbial biomass' or 'microbial/active N,' is the living portion of the soil organic matter, excluding plant roots and soil animals larger than 5 x 10^{-3} μm^3. Although, microbial biomass constitutes a small portion of organic matter (~ 2%), it is central in microbial activity, in other words conversion of organic N to inorganic N (Cameron and Moir, 2013; Manzoni and Porporato, 2009). The transformation rate of organic N to microbial N is controlled by the relative C and N content in microbial biomass, soil temperature and water content, soil silt and clay content, organic residue composition- enhanced by tillage in agricultural soil, bulk density, oxygen content, and inorganic N availability. Microbial N has quicker turnover times ranging from days to weeks compared to hundreds of years for slow or passive organic matter (Izaurralde et al., 2006; Schimel and Weintraub, 2003). Hence, microbial biomass is the main clearinghouse and driver of C and N cycling in EPIC. Whether net mineralization of organic N to NH_4^+ occurs or net immobilization of NO_3^- to microbial N depends strongly on the relative C and N contents in microbial biomass. Higher N content supports net mineralization, whereas higher C content supports net immobilization. C and N can also be leached or lost in gaseous forms (Izaurralde et al., 2012).

We then estimate gaseous N emissions by using the organic N, NH_4, NO_3, and C pools provided from EPIC/FEST-C along with relevant soil properties for agricultural biomes from the DayCENT nitrification and denitrification sub-model, as described in Section 2.6.4 and illustrated in Figure 2.

2.6.3 Non-agricultural regions

We adapt the framework for linked C and N cycling from Schimel and Weintraub (2003) for non-agricultural regions, where EPIC is not applicable. This framework accounts for the mineralization of organic N by considering which element is limiting based on relative C to N content in microbial biomass. If N is in excess, then mineralization of organic N producing NH_4^+ is favored. If C is in excess, it results in overflow metabolism that results in elevated C respiration rates that are not associated with microbial growth. The resultant inorganic N and C respiration rates are then applied on a temporal and spatial scale consistent with those for the EPIC agricultural pool.

To ensure mass balance, enzyme production (Equations 11-13) and recycling mechanisms (Equations 14-15) to replenish microbial biomass C are crucial. Similarly, net immobilization is assumed as was done in EPIC, when we approach C saturated conditions with time to replenish microbial N. Without such mechanisms, there is a danger to always incorrectly predict N or C-limited state for microbes. Also, some proportion of the microbial biomass is utilized for maintenance of living cells (only C demand) (Equation 14), while the rest accounts for decay and regrowth (both C and N demands) (Equations 16-17, 18-19) (Schimel and Weintraub, 2003; Manzoni and Porporato, 2009). Fractions of C and N in dying microbial biomass are recycled into the available microbial C and N pools. Schimel and Weintraub (2003) provide values for parameters that quantify these growth and decay processes: Fraction of Biome C to exoenzymes (K_e) = 0.05; microbial maintenance rate (K_m) = 0.01 d^{-1}; substrate use efficiency (SUE) = 0.5; Proportion of microbial biomass that dies per day (K_t) = 0.012 d^{-1}; Proportion of microbial biomass (C or N) for microbial use (K_r) = 0.85.

$$R_m\ (Respiration\ from\ maintenance) = \mathrm{K}_m(SMC) \quad (10)$$

$$R_e\ (Respiration\ from\ enzyme\ production) = ((1 - \mathrm{SUE})(EP_C)/SUE) \quad (11)$$

$$EP_C\ (Enzyme\ production\ as\ C\ Loss/Sink) = \mathrm{K}_e(SMC) \quad (12)$$

EP_N $(Enzyme\ production\ as\ N\ Loss/Sink) =$
$EP_C/3$ $(Where\ 3\ is\ the\ approximate\ C{:}N\ ratio\ for\ protien)$ (13)

CY_C $(Recycle\ from\ C\ microbial\ biomass) = \mathrm{K}_t\mathrm{K}_r(SMC)$ (14)

CY_N $(Recycle\ from\ N\ microbial\ biomass) = CY_C/C_m{:}N_m$ (15)

H_C $(C\ Death/decay) = \mathrm{K}_t(1 - \mathrm{K}_r)(SMC)$ (16)

H_N $(N\ Death/decay) = H_C/C_m{:}N_m$ (17)

$If\ C\ limited\ or\ N\ in\ excess$:

$SMC < R_m + (EP_C/SUE) + \big((SMN - EP_N)(C_m{:}N_m/SUE)\big)$ (18)

R_g $(Respiration\ from\ growth,\ C\ limited) = (1 - \mathrm{SUE})(SMC - (EP_C/SUE) - R_m)$ (19)

R_O $(Respiration\ from\ overflow\ mechanism)$ = 0 (20)

NH_4 $(From\ net\ mineralization\ after\ mass\ balance)$ = $(SMN - EP_N - ((SMC - (EP_C/SUE) - R_m)(SUE/C_m{:}N_m)))$ (21)

We represent spatial heterogeneity in soil C and N by using the Schimel and Weintraub (2003) algorithm with sub-grid land use fractions from NLCD40 to estimate the different parameters for specific non-agricultural biomes in Equations 10-20. That allows us to account for inter-biome variability in soil properties and organic/microbial biomass.

Mineralized N pools generated as NH_4^+ in this framework are calculated eventually as a function of microbial biomass and aforementioned parameters driving the net mineralization (Equations 18 and 21).

We map a global organic C and N pool dataset (Xu et al., 2015) onto our CONUS domain, using biome-specific fractions from 12 different biome types for conversion of these organic pools into microbial biomass pools (Xu et al., 2013). We map these 12 broader biome types to the 24 MODIS biome types by the mapping shown in Table A1. To ensure consistency with the sub-grid biome fractions for the 40 NLCD biome types (section 2.2), we map the MODIS 24 biome-specific microbial/Organic C and N fractions to NLCD 40 ($Cmic_{biome}$ and$Nmic_{biome}$, $biome$ represents the 40 NLCD categories) by the mappings shown in Tables A2 and A3. We calculate area-weighted microbial C and N pools ($SMC\ and\ SMN$) using $Cmic_{biome}$ and $Nmic_{biome}$ that account for the inter-biome variability in availability of soil microbial biomass. Also, spatial heterogeneity in terms of vertical stratification is crucial as emission losses from N cycling primarily happen in the top 30-cm layer. Hence we incorporate the Xu et al. (2015) data for the top 30 cm for organic nutrient pool and microbial C:N ratio ($C_m: N_m$) along with other soil properties such as soil pH, θ_{soil}, and T_{soil}. This framework (Figure 2) enables us to estimate soil NH_4, NO_3, and C pools from area-weighted microbial biomass as consistently as possible with the pools that EPIC provides in agricultural regions.

2.6.4 DayCENT representation of soil N emissions

The final part of the mechanistic framework is formed by using a nitrification and denitrification N emissions sub-model adapted from DayCENT along with nitrification and denitrification rate calculations adapted from EPIC. Nitrification and denitrification rates are adapted from EPIC to maintain consistency with NH_3 bi-directional scheme in CMAQ, which uses the same. It should be noted that the coupled C–N decomposition module in the EPIC terrestrial ecosystem model is similar to that of DayCENT (Izaurralde et al., 2012; Izaurralde et al., 2017; Gaillard et al., 2017). EPIC simulated agricultural NH_4 and NO_3 soil pools are generated as described in Section 2.6.2, whereas the non-agricultural NH_4 and NO_3 soil pools are calculated by the methods described in Section 2.6.3 (Equations 22-23). NH_4 and NO_3 soil pools drive nitrification and denitrification as shown in Equations 24-25. Variability in terms of soil conditions influencing N emissions in nitrification and denitrification are introduced through the rates at which NH_4 is nitrified (R_N) and NO_3 is denitrified (R_D) (Equations 24-25).

The nitrification rate (K_N) (Equation 26) is estimated based on regulators from the soil water content, soil pH, and soil temperature (T_{soil}), following the approach of Williams et al. (2008), consistent with the bi-directional NH_3 scheme in CMAQ (Bash et al., 2013). The nitrification soil temperature regulator (f_T) accounts for frozen soil with no evasive N fluxes (Equation 27). The nitrification soil water content regulator (f_{SW}) accounts for soil water content at wilting point and field capacity (Equations 28-29). The regulator terms f_T and f_{SW} both get their dependent variables from Meteorology-Chemistry Interface Processor (MCIP) (Otte and Pleim, 2010) derived land-surface outputs. However the nitrification soil pH regulator (f_{pH}) takes soil pH for agriculture soil from EPIC and for non-agricultural soil from a separate global dataset (Xu et al., 2015), available at both 0.01 m and 1 m depths to maintain consistency with MCIP (Equation 30). Denitrification rate (K_D) (Equation 31) is regulated by soil temperature (Equation 34), with WFPS (Equation 33) acting as a proxy for O_2 availability and soil moisture (θ_{soil}), and relative availability of NO_3 and C (Equation 32) determining N_2O or N_2 emissions during denitrification (Williams et al., 2008). Note that Equations 26 and 31 set upper limits for K_N and K_D, respectively.

$$NO_3(kg-N/ha\,, after\ Nitrification) = NH_4\,(1.0 - e^{-(K_N dt)}) \quad (22)$$

$$NH_4\,(kg-N/ha\,, after\ Nitrification) = NH_4\ e^{-(K_N dt)} \quad (23)$$

$$R_N\,(kg-N/ha\ per\ s) = NH_4\,(1.0 - e^{-(K_N dt)})/dt \quad (24)$$

$$R_D\,(kg-N/ha\ per\ s) = NO_3\,(1.0 - e^{-(K_D dt)})/dt \quad (25)$$

$$K_N\,(s^{-1}) = min\big(0.69, (f_T)\,(f_{SW})(f_{pH})\big) \quad (26)$$

$$f_T(\text{Nitrification soil temperature regulator}) = max(0.041(T_{soil} - 278.15), 0.0) \quad (27)$$

f_{SW} (Nitrification soil water content regulator)

$$= \begin{cases} 0.1, \quad If\ (\theta_{soil} \le wilting\ point) \\ \max\left(0.1, 0.1 + 0.9\sqrt{\dfrac{(\theta_{soil} - wilting\ point)}{(field\ capacity - wilting\ point)}}\ , \dfrac{(\theta_{soil} - wilting\ point)}{0.25\,(field\ capacity - wilting\ point)}\right), \\ If\ (wg25 > \theta_{soil} > wilting\ point) \\ 1.0, \quad If\ (field\ capacity > \theta_{soil} \ge wg25) \\ max\left(0.1, 1.0 - \dfrac{(\theta_{soil} - field\ capacity)}{(\theta_{soil}(at\ Saturation) - field\ capacity)}\right), \quad If\ (\theta_{soil} > field\ capacity) \end{cases} \quad (28)$$

$$wg25 = wilting\ point + 0.25\,(field\ capacity - wilting\ point) \quad (29)$$

f_{pH} (Nitrification soil pH regulator)

$$= \begin{cases} 0.307(pH) - 1.269, & Acidic\ soil\ (pH < 7) \\ 1.0, & Neutral\ soil\ (7.4 > pH \ge 7) \\ 5.367 - 0.599(pH), & Alkaline\ soil\ (pH \ge 7.4) \end{cases} \quad (30)$$

$$K_D\,(s^{-1}) = min(0.01, f(WFPS, T_{soil}, NO_3{:}C)) \quad (31)$$

$$f(WFPS, T_{soil}, NO_3 : C), \text{Denitrification regulators}$$

$$= (f_{T,D})\,(f_{WFPS,D})\left(\frac{\big(1.4\,(LabileC)(NO_3)\big)}{\big((LabileC + 17\,)(NO_3 + 83)\big)}\right) \quad (32)$$

$$f_{WFPS,D} = \min\left(1.0, \frac{4.82}{14^{(\,16/(12^{\,(1.39\,(WFPS))})\,)}}\right) \quad (33)$$

$$f_{T,D} = min\left(1.0, e^{\left(308.56\left(\frac{1}{68.02}-\frac{1}{T_{soil\,(in\,K)}-227.13}\right)\right)}\right) \quad (34)$$

DayCENT partitions N emissions as NO_x and N_2O based on relative gas diffusivity in soil compared to air (Dr) (Equation 35). Dr is calculated based on the algorithm from Moldrup et al. (2004), which accounts for soil water content, soil air porosity, and soil type. Also, Dr and hence the ratio of NO_x to N_2O emissions (r_{NOx/N_2O}) being a function of Dr, accounts for soil texture by quantifying pore space, which is highest in coarse soil (Parton et al., 2001; Moldrup et al., 2004). DayCENT assumes 2% of nitrified N (R_N) is lost as N_2O (Equation 36). r_{NOx/N_2O} is the ratio of NO_x (both NO and HONO, which photolyses rapidly to NO) to N_2O, where emissions are expressed on g-N/hr basis. These emissions are susceptible to pulsing after re-wetting of soil in arid or semi-arid conditions ($P\big(l_{dry}\big)$, as explained in section 2.1 (Equation 37). Denitrification NO is also calculated using the overall r_{NOx/N_2O} ratio (Equation 38) but does not experience pulsing (Parton et al., 2001). Equation 35 does quantify r_{NOx/N_2O} as a function of Dr, but as a unitless ratio as expected.

$$r_{NOx/N_2O} = 15.2 + \left(\frac{35.5\,arctan\big(0.68\,\pi\,((10.0\,Dr)-1.86)\big)}{\pi}\right) \quad (35)$$

$$N_{N_2O}\ (Nitrification\ N_2O, g - N/hr) = 0.02\,(R_N)(Grid\ cell\ area) \quad (36)$$

$$N_{NO_x}(Nitrification\ NO_x, g - N/hr) = r_{NOx/N_2O}(N_{N_2O})\,P\big(l_{dry}\big) \quad (37)$$

$$D_{NO}\ (Denitrification\ NO, g - N/hr) = r_{NOx/N_2O}\,(D_{N_2O}) \quad (38)$$

N_2O from denitrified NO_3 (R_D) is calculated using the partitioning function derived by Del Grosso et al. (2000) (Equation 39). The ratio of N_2 to N_2O emitted as an intermediate during denitrification (r_{N_2/N_2O}) is dependent on WFPS (Equation 42) and the relative availability of NO_3 substrate and

C for heterotrophic respiration (Equations 40-41). The C available for heterotrophic respiration in the surface soil layer ($LabileC$) (Equation 41) is taken from EPIC for agricultural biomes and from Xu et al. (2015) for non-agricultural biomes. $f(NO_3{:}C)$ is controlled by variability in soil texture, accounted by a factor k, which depends on soil diffusivity at field capacity as estimated in Del Grosso et al. (2000). Also, the NO_3 pool is updated at each time step when denitrification happens (Equation 43). Equations 40-42 also quantify r_{N_2/N_2O} as a unitless ratio, while still accounting for variables influencing these ratios.

$$D_{N_2O}\ (Denitrification\ N_2O, g-N/hr) = \left(\frac{R_D}{1.0 + r_{N_2/N_2O}}\right) (Grid\ cell\ area) \qquad (39)$$

$$r_{N_2/N_2O} = f(NO_3{:}C)\, f(WFPS) \qquad (40)$$

$$f(NO_3{:}C) = \begin{cases} max\left(0.16\ (k), (k)e^{-0.8\ \left(\frac{NO_3}{LabileC}\right)}\right) & , if\ LabileC > 0 \\ 0.16\ (k) & , if\ LabileC \sim 0 \end{cases} \qquad (41)$$

$$f(WFPS) = max\left(\ 0.1, (0.015\ (WFPS(as\ fraction) - 0.32))\right) \qquad (42)$$

$$NO_3\ (kg-N/ha, after\ denitrification) = \frac{R_N}{K_D} + \left(NO_3 - \frac{R_N}{K_D}\right)(e^{-(K_D dt)}) \qquad (43)$$

HONO is emitted as an intermediate during nitrification, and has been reported in terms of a ratio relative to NO for each of 17 ecosystems by Oswald et al. (2013). In the mechanistic scheme, the proportions of HONO relative to total NO_x for these 17 biomes were mapped to the closest 24 MODIS type biome categories (Table A1) and then to the NLCD 40 types ($HONO_f$) by the mappings in Tables A2 and A3. This allows consistency with sub-grid land use fractions from NLCD40. HONO emissions are further adjusted to reflect their dependence on WFPS (Oswald et al., 2013). The adjustment factor f_{SWC} reflects observations that HONO emissions rise linearly up to 10% WFPS and then decrease until they are negligible around ~ 40% (Su et al., 2011; Oswald et al., 2013) (Equation 45). Subsequently, total NO emission is a sum of nitrification NO emission, which is a difference of N_{NO_x} and S_{HONO}, and denitrification NO (Equation 46). Similarly, total N_2O is a sum of N_{N_2O} (Equation 36) and D_{N_2O} (Equation 39). The canopy reduction factor (section 2.1) is then applied to both S_{HONO} and S_{NO} (Equations 44 and 46). Finally, sub-grid scale emission rates are aggregated for each grid cell.

$$S_{HONO} = (HONO_f)(N_{NO_x})\,(f_{SWC})CRF(LAI, Meteorology, Biome) \qquad (44)$$

f_{SWC}(Soil water content adjustment factor to compute HONO)

$$= \begin{cases} \dfrac{(HONO_f)(WFPS)}{0.1}, & If\ (WFPS \le 0.10) \\ (Assuming\ linear\ increase\ up\ to\ 10\%\ WFPS) & \\ \dfrac{(HONO_f)(0.4 - WFPS)}{(0.4 - 0.1)}, & If\ (WFPS \le 0.40) \\ 0, & If\ (WFPS > 0.40) \end{cases} \qquad (45)$$

$$S_{NO} = \Big\{\Big(N_{NO_x} - \big(\,(HONO_f)(N_{NO_x})\,(f_{SWC})\,\big)\Big) + D_{NO}\Big\}CRF(LAI, Meteorology, Biome) \qquad (46)$$

2.7 Model configurations

We obtained from U.S. EPA a base case WRFv3.7-CMAQv5.1 simulation for 2011 with the settings and CONUS modeling domain described by Appel et al. (2017), who thoroughly evaluated its performance against observations. Here, we simulate only May and July to test sensitivity of air pollution to soil N emissions during the beginning and middle of the growing season. Each episode is preceded by a 10-day spin-up period.

Table 2 summarizes the WRF-CMAQ modeling configurations settings. The simulations use the Pleim-Xiu Land Surface Model (PX-LSM) (Pleim and Xiu, 2003) and the Asymmetric Convective Mixing v2 (ACM2) Planetary Boundary Layer (PBL) model. The modeling domain for CMAQ v5.1 covers the entire CONUS including portions of northern Mexico and southern Canada with 12-km resolution and a Lambert Conformal projection. Vertically, we use 35 vertical layers of increasing thickness extending up to 50 hPa. Boundary conditions are provided by a 2011 global GEOS-Chem simulation (Bey et al., 2001).

WRF simulations employed the same options as Appel et al. (2017) (Summarized in Table 2). WRF outputs for meteorological conditions were converted to CMAQ inputs using MCIP version 4.2 (https://www.cmascenter.org). Gridded speciated hourly model-ready emissions inputs were generated using Sparse Matrix Operator Kernel Emissions (SMOKE; https://www.cmascenter.org/smoke/) version 3.5 program and the 2011 National Emissions Inventory v1. Biogenic emissions were processed in-line in CMAQ v5.1 using BEIS version 3.61 (Bash et al., 2016). All the simulations employed the bidirectional option for estimating the air–surface exchange of ammonia. We applied CMAQ with three sets of soil NO emissions: a) standard YL soil NO scheme in BEIS; b) updated BDSNP scheme for NO (Rasool et al., 2016) with new sub-grid biome classification; and c) mechanistic soil N scheme for NO and HONO.

2.8 Observational data for model evaluation

To evaluate model performance for each of the three soil N cases, we employed regional and national networks: EPA's Air Quality System (AQS; 2086 sites; https://www.epa.gov/aqs) for hourly NO_x and O_3; the Interagency Monitoring of Protected Visual Environments (IMPROVE; 157 sites; http://vista.cira.colostate.edu/improve/) and Chemical Speciation Network (CSN; 171 sites; https://www3.epa.gov/ttnamti1/speciepg.html) for $PM_{2.5}$ nitrate (measured every third or sixth day); the Clean Air Status and Trends Network (CASTNET; 82 sites; http:// www.epa.gov/castnet/) for hourly O_3 and weekly aerosol PM species; and SEARCH network measurements (http://www.atmospheric-research.com/studies/SEARCH/index.html) of NO_x concentrations in remote areas. NO_2 was also evaluated against tropospheric columns observed by the Ozone Monitoring Instrument (OMI) aboard NASA's Aura satellite (Bucsela et al., 2013; Lamsal et al., 2014).

3 Results and Discussion

3.1 Spatial distribution of soil NO, HONO and N_2O emissions

Figure 3 compares the spatial distribution of soil N oxide emissions from the three schemes. The incorporation of EPIC fertilizer in BDSNP results in soil NO emission rates up to a factor of 1.5 higher than in YL, consistent with the findings of Rasool et al. (2016). Hudman et al. (2012) found nearly twice as large of a gap between BDSNP and YL in GEOS-Chem; the narrower gap here likely results from our use of sub-grid biome classification and EPIC fertilizer data (Rasool et al., 2016). The mechanistic scheme (Figure 3c) generates emission estimates that are closer to the YL scheme but with greater spatial and temporal heterogeneity, reflecting its use of more dynamic soil N and C pools. The agricultural plains extending from Iowa to Texas with high fertilizer application rates have the highest biogenic NO and HONO emission rate, with obvious temporal variability between May and July (Figure 3). In all of the schemes, soil N represents a substantial fraction of total NO_x emissions over many rural regions, especially in the western half of the country (Figure S1). However, the aggregated budget of soil NO is much less than anthropogenic NO_x from ~~fossil fuels~~non-soil related sources, because ~~anthropogenic emissions are~~fossil fuel use is concentrated in a limited number of urbanized and industrial locations. The percentage contribution of soil NO to total NO_x aggregated across the CONUS domain varied for May-July between: 15-20% for YL, 20-33% for updated BDSNP, and 10-13% for mechanistic schemes respectively.

Direct observations of soil emissions are sparse and most were reported decades ago. While the meteorological conditions will differ, these observations give us the best available indicator of the ranges of magnitudes of emission rates actually observed in the field. The sites encompass a variety of fertilized agricultural fields and fertilized and unfertilized grasslands (Bertram et al., 2005; Hutchinson and Brams, 1992; Parrish et al., 1987; Williams et al., 1991; Williams et al., 1992; Martin et al., 1998). For fair comparison, peak location/site was selected across a range of sites for a specific observation study and compared to respective peak modeled value across sites/grids in the same spatial domain. Also, for comparison with natural unfertilized grassland observational studies based in Colorado, modeled estimates from non-agricultural grids only were selected. Overall, the YL scheme and the mechanistic scheme produce emissions estimates that are roughly consistent with the ranges of emission rates observed at each site (Table 3). By contrast, BDSNP tends to overestimate soil NO compared to these observations (Table 3).

Table 3 also shows opposing trends for May and July soil NO estimates between YL or BDSNP and mechanistic schemes for Iowa and South Dakota fertilized fields that make up the significant part of corn-belt in U.S. For these regions, soil NO tends to be higher in July than in May in YL and BDSNP, but lower in July in the mechanistic scheme (Table 3). The U.S. Corn Belt has the most synthetic N fertilizer application in April (Wade et al., 2015), which can explain the high soil NO emissions in May that decline in July. N_2O emissions have been particularly observed to be highest during May-June after April N fertilizer application in the U.S. Corn Belt, and declining thereafter (Griffis et al., 2017). This is further confirmed in our estimates for soil N_2O emissions from mechanistic scheme, where May estimates are higher than in July and the maximum emissions are observed in the Iowa Corn Belt (Figure 4). However, unlike NO_x emissions, for N_2O no background conditions or emission inventory is in place in CMAQ's chemical transport model, so comparisons with ambient observations are not yet possible.

3.2 Evaluation with $PM_{2.5}$, ozone, and NO_x observations

Model results with the three soil N schemes are compared with observational data from IMPROVE and CSN monitors for $PM_{2.5}$ NO_3 component, AQS monitors for NO_x and ozone, and CASTNET monitors for ozone. Both YL and the new mechanistic schemes exhibit similar ranges of biases for these pollutants (see Figures S2, S3, S4, S5 and S6 in supplementary material). Use of the mechanistic scheme in place of YL changes soil N emissions by less than 25 ng-N m^{-2} s^{-1} in most regions, corresponding to NO_x concentration changes of less than 1 ppb (Figure 5). CASTNET and IMPROVE monitors tend to be more remote than AQS and CSN monitors, many of which are located in urban regions.

At AQS monitors, switching between soil N schemes changes MB for O_3 by up to ~ 1.5 ppb (Figure 6), whereas absolute MB of models versus observations is up to ~ 10 ppb (Figure S2). For NO_x, the maximum difference in MB between soil N schemes is ~ 0.4 ppb (Figure 7), compared to maximum absolute MB of ~ 10 ppb between model and observations (Figure S3). For CASTNET monitors, the differences in MB for O_3 between soil N schemes can reach a maximum of ~ 1.5 ppb (Figure 8), compared to 6 ppb maximum absolute MB of models versus observations (Figure S4). Similarly, for IMPROVE $PM_{2.5}$ NO_3, maximum difference in MB between soil N schemes is ~ 0.06 μg/m^3 (Figure 9), compared to maximum absolute MB of 0.4 μg/m^3 (Figure S5). For CSN $PM_{2.5}$ NO_3, the maximum MB difference between soil N schemes is ~ 0.1 μg/m^3 (Figure 10), compared to maximum absolute MB of ~ 50 μg/m^3 (Figure S6). Similar trends are observed for both May and July as illustrated in Figures 6-10.

Overall, the mechanistic scheme tends to reduce CMAQ's positive biases for pollutants across the Midwest and eastern US, whereas BDSNP worsens overestimations in these regions for both May and July 2011 (Figures 6-10). In addition, negative bias in difference means less bias compared to observation (Figures 6-10). One reason for the differences is that the mechanistic scheme recognizes dry conditions in unirrigated fields in these regions, whereas the low WFPS threshold in BDSNP (θ = 0.175 (m^3/m^3)) treats most of these regions as wet and thus higher emitting.

3.2.1 Evaluation with South Eastern Aerosol Research and CHaracterization (SEARCH) Network NO_x measurements

We analyzed how the choice of soil NO parameterization affects NO_x concentrations in non-agricultural regions by using SEARCH network measurements (http://www.atmospheric-research.com/studies/SEARCH/index.html). Six SEARCH sites located in the southeastern U.S. are evaluated for May and July 2011: Gulfport, Mississippi (GFP) urban coastal site ~1.5 km from the shoreline, Pensacola – outlying (aircraft) landing field (OLF) remote coastal site near the Gulf ~20 km inland, Atlanta, Georgia–Jefferson Street (JST) and North Birmingham, Alabama (BHM); both urban inland sites, and Yorkville, Georgia (YRK) and Centreville, Alabama (CTR), remote inland forest sites.

Across the southeastern U.S. during these episodes, BDSNP estimated higher emissions than YL and the mechanistic scheme estimated lower emissions (Figure 3). Also, CMAQ with each scheme overestimated NO_x observed at each SEARCH site (Figure 11). Thus, shifting from YL to BDSNP worsens mean bias (MB) for NO_x, while the mechanistic scheme reduces MB. The impacts are most pronounced at the rural Centerville site (Figure 11).

3.3 Evaluation with OMI satellite NO_2 column observations

Tropospheric NO_2 columns observed by OMI and available publicly at the NASA archive (http://disc.sci.gsfc.nasa.gov/Aura/data-holdings/OMI/omno2_v003.shtml; Bucsela et al., 2013; Lamsal et al., 2014) are used to evaluate the performance of CMAQ under the three soil NO_x schemes. To enable a fair comparison, the quality-assured/quality-checked (QA/QC) clear-sky (cloud radiance fraction < 0.5) OMI NO_2 data are gridded and projected to our CONUS domain using ArcGIS 10.3.1. CMAQ NO_2 column densities in molecules per cm^2 are generated from CMAQ through vertical integration using the variable layer heights and air mass densities in these tropospheric layers. These NO_2 column densities are then extracted for 13:00-14:00 local time across the CONUS domain, to match the time of OMI overpass measurements.

We compared CMAQ simulated tropospheric NO_2 columns with OMI data for four broad regions that showed the highest sensitivity to the soil N schemes. For May 2011, the mechanistic scheme produces higher estimates of NO_2 than YL in the western U.S. and Texas, and lower estimates in the rest of the agricultural Great Plains. In July however, the mechanistic scheme produces lower estimates than YL in each of these regions, but the differences are narrower than in May (Figure 12). Switching from YL to our updated mechanistic scheme improved agreement with OMI NO_2 columns in the western U.S. (for May only), Montana, North and South Dakota, North and South Carolina and Georgia (July only), and Oklahoma and Texas (red boundaries). However, switching from YL to mechanistic scheme worsens underpredictions of column NO_2 in the rest of the Midwest (black boundaries) during both May and July (Figures 12 and 13). The mechanistic scheme improves model performance in the southeastern U.S. and many portions of the central and western U.S. (Table 4). Overestimation is exhibited for the eastern U.S. across all soil N schemes and can be attributed more to the current emission inventory in CMAQ overestimating NO_2 vertical column density in this region of CONUS (Kim et al., 2016). For Texas and Oklahoma, the mechanistic scheme performs better than YL but still underestimates OMI observations in May, and performs well in July (Figure 13).

Underestimates of soil N in some regions with an abundance of animal farms, such as~~,~~ parts of Colorado, New Mexico, ~~N~~north Texas, California, the ~~N~~northeast U.S. and the Midwest~~:~~, may be attributed to the lack of representation of farm-level manure N management practices, in which manure application can exceed the EPIC estimate of optimal crop demand. Farms in the vicinity of concentrated animal units often apply N in excess of the crop N requirements as part of the manure management strategy, typically increasing the N emissions (Montes et al., 2013). USDA has reported that confined animal units/livestock production correlates with increasing amounts of farm-level excess N (Kellogg et al., 2000; Ribaudo and Sneeringer, 2016). Model representations of these practices are needed to better estimate the impact of nitrogen in the environment.

4 Conclusions

Our implementation of a mechanistic scheme for soil N emissions in CMAQ provides a more physically based representation of soil N than previous parametric schemes. To our knowledge, this is the first time that soil biogeochemical processes and emissions across a full range of nitrogen compounds have been simulated in a physically realistic manner in a regional photochemical model. Our mechanistic scheme directly simulates nitrification and denitrification processes, allowing it to consistently estimate soil emissions of NO, HONO, NH_3, and N_2O (Figures 1 and 2). The mechanistic scheme also updates the representation of the dependency of soil N on WFPS by utilizing parameters like water content at saturation, wilting point, and field capacity and their impact on gas diffusivity (Del Grosso et al., 2000; Parton et al., 2001).

Overall, the magnitudes of soil NO_x emissions predicted by the mechanistic scheme are similar to those predicted by the YL parametric scheme, and smaller than those predicted by the BDSNP scheme. In dry conditions, soil NO has been shown to be highest as compared to wet conditions with lowest, explained by sustained high nitrification rates due to high gas diffusivity in dry conditions (Homyak et al., 2014). Arid soils or dry season with adequate soil N due to asynchrony between soil C mineralization and nitrification have been shown to shut down plant N uptake through high gas diffusivity, causing NO emissions to increase (Evans and Burke, 2013; Homyak et al., 2016). Mechanistic scheme exhibits this spatial variability in soil NO depending on dry or wet conditions, since it accounts for their dependence on soil moisture and gas diffusivity, as well as the C and N cycling that leads to adequate soil N.

Spatial patterns of NO_x emissions differ across the schemes and episodes (Figure 3), but generally show highest emissions in fertilized agricultural regions. During the episodes considered here, Texas experienced severe to extreme drought, while parts of the Northeast and Pacific Northwest were unusually wet (http://www.cpc.ncep.noaa.gov/products/analysis_monitoring/regional_monitoring/palmer/2011/). Testing for other time periods is needed to see how results differ during different seasons and as drought conditions vary. Model evaluation will also depend on the meteorological model's skill in capturing dry and wet conditions.

The lower emissions of the mechanistic scheme reduce the overprediction biases for ground-based observations of ozone and PM nitrate that had been reported by Rasool et al. (2016) for the BDSNP scheme (Figures 6-10). The mechanistic scheme reduced overpredictions of NO_x concentrations at SEARCH sites in the southeastern U.S. (Figure 11). However, changes in performance for simulating satellite observations of NO_2 columns were mixed (Figures 12-13). The underestimation of NO_2 by CMAQ with the mechanistic scheme in agricultural regions of the Midwest may be partially attributed to neglecting manure management practices from livestock operations. In the U.S., 60 percent of Nitrogen from manure produced on animal feedlot operations cannot be applied to their own land because they are in 'excess' of USDA advised agronomic rates. Most U.S. counties with animal farms have adequate crop acres not associated with animal operations, but within the county, on which it is feasible to spread the excess manure at agronomic rates at certain additional cost. However, 20 percent of the total U.S. on-farm excess manure nitrogen is produced in counties with insufficient cropland for its application at agronomic rates (Gollehon et al., 2001). For areas without adequate land, alternatives to local land application such as energy production (for example, biofuel) are needed. In absence of such a mitigation strategy, excess manure N applied on soil contributes is susceptible to reactive N emissions and leaching (Ribaudo et al., 2003; Ribaudo et al., 2012).

Although this work represents the most process-based representation of soil N ever introduced to a regional photochemical model, limitations remain. EPIC still lacks complete representation of farming management practices like excess N applied as part of nutrient management from livestock, which can increase soil N pools and associated emissions. Developing and evaluating these models to addresses management decisions is challenging as they are often regionally specific and based on expert knowledge including regional and global economics and biogeochemical processes that have yet to be codified into a predictive system. Some aspects of soil N biogeochemistry remain insufficiently understood, especially as they relate to HONO emissions. Nevertheless, the mechanistic approach introduced here will make it possible to incorporate future advancements in understanding C and N cycling processes.

For future work, there is a need for more accurate representation of actual farming practices beyond the generalizations made by the EPIC model. Model development should be continued to better constrain N sources such as rock weathering, which are still ignored for estimating soil N emissions. Recently, Houlton et al. (2018) postulated that bedrock weathering can contribute an additional 6-17 % to global inorganic soil N for different natural biomes. There is also a need for more field observations of soil N emissions to better evaluate the spatial and temporal patterns simulated by the models.

Code availability

The modified and new source code, inputs, and sample outputs along with the user manual giving details on implementing the new mechanistic module in-line with CMAQ Version 5.1, as used in this work are available on the Oak Ridge National Laboratory Distributed Active Archive Center for Bio-geochemical Dynamics (Rasool et al., 2018; https://doi.org/10.3334/ORNLDAAC/1661). Source codes for CMAQ version 5.1 and FEST-C version 1.2 are both open-source, available with applicable free registration at http://www.cmascenter.org. Advanced Research WRF model (ARW) version 3.7 used in this study is also available as a free open-source resource at http://www2.mmm.ucar.edu/wrf/users/download/get_source.html.

Author contribution

Quazi Rasool developed the model code with Jesse Bash. Quazi Rasool performed the simulations and analysis. Quazi Rasool prepared the manuscript with extensive reviews and edits from Jesse Bash and Daniel Cohan.

Acknowledgements

NASA (grant number NNX15AN63G) provided the funding for this work. We acknowledge Dr. Ellen Cooter from U.S. EPA for her insights and invaluable help with EPIC/FEST-C modeling. The views expressed in this article are those of the authors and do not necessarily reflect the views or policies of the U.S. Environmental Protection Agency.

References

Appel, K. W., Napelenok, S. L., Foley, K. M., Pye, H. O., Hogrefe, C., Luecken, D. J., Bash, J. O., Roselle, S. J., Pleim, J. E., and Foroutan, H.: Description and evaluation of the Community Multiscale Air Quality (CMAQ) modeling system version 5.1, Geoscientific Model Development, 10, 1703, 2017.

Barton, L., McLay, C., Schipper, L., and Smith, C.: Annual denitrification rates in agricultural and forest soils: a review, Soil Research, 37, 1073-1094, 1999.

Bash, J. O., Baker, K. R., and Beaver, M. R.: Evaluation of improved land use and canopy representation in BEIS v3. 61 with biogenic VOC measurements in California, Geoscientific Model Development, 9, 2191, 2016.

Bash, J., Cooter, E., Dennis, R., Walker, J., and Pleim, J.: Evaluation of a regional air-quality model with bidirectional NH 3 exchange coupled to an agroecosystem model, Biogeosciences, 10, 1635-1645, 2013.

Bertram, T. H., Cohen, R. C., Thorn III, W. J., and Chu, P. M.: Consistency of ozone and nitrogen oxides standards at tropospherically relevant mixing ratios, Journal of the Air & Waste Management Association, 55, 1473-1479, 2005.

Bey, I., Jacob, D. J., Yantosca, R. M., Logan, J. A., Field, B., Fiore, A. M., Li, Q., Liu, H., Mickley, L. J., and Schultz, M.: Global modeling of tropospheric chemistry with assimilated meteorology: Model description and evaluation, J. Geophys. Res., 106, 23,073-23,096, 2001.

Bucsela, E. J., Krotkov, N. A., Celarier, E. A., Lamsal, L. N., Swartz, W. H., Bhartia, P. K., Boersma, K. F., Veefkind, J. P., Gleason, J. F., and Pickering, K. E.: A new stratospheric and tropospheric NO2 retrieval algorithm for nadir-viewing satellite instruments: applications to OMI, Atmos. Meas. Tech., 6, 2607-2626, doi:10.5194/amt-6-2607-2013, 2013.

Butterbach-Bahl, K., Baggs, E. M., Dannenmann, M., Kiese, R., and Zechmeister-Boltenstern, S.: Nitrous oxide emissions from soils: how well do we understand the processes and their controls?, Phil. Trans. R. Soc. B, 368, 20130122, 2013.

Cameron, K., Di, H. J., and Moir, J.: Nitrogen losses from the soil/plant system: a review, Annals of Applied Biology, 162, 145-173, 2013.

Conrad, R.: Microbiological and biochemical background of production and consumption of NO and N 2 O in soil. In: Trace gas exchange in forest ecosystems, Springer, 2002.

Cooper, O.R., Parrish, D.D., Ziemke, J., Balashov, N.V., Cupeiro, M., Galbally, I.E., Gilge, S., Horowitz, L., Jensen, N.R., Lamarque, J.F. and Naik, V.: Global distribution and trends of tropospheric ozone: An observation-based review. Elementa: Science of the Anthropocene, 2(1), p.000029, 2014.

Cooter, E., Bash, J., Benson, V., and Ran, L.: Linking agricultural crop management and air quality models for regional to national-scale nitrogen assessments, Biogeosciences, 9, 4023-4035, 2012.

Davidson, E. A. and Verchot, L. V.: Testing the Hole-in-the-Pipe Model of nitric and nitrous oxide emissions from soils using the TRAGNET Database, Global Biogeochemical Cycles, 14, 1035-1043, 2000.

Davidson, E. and Kingerlee, W.: A global inventory of nitric oxide emissions from soils, Nutr. Cycl. Agroecosys., 48, 37–50, doi:10.1023/A:1009738715891, 1997.

Davidson, E., David, M. B., Galloway, J. N., Goodale, C. L., Haeuber, R., Harrison, J. A., Howarth, R. W., Jaynes, D. B., Lowrance, R. R., and Thomas, N. B.: Excess nitrogen in the US environment: trends, risks, and solutions, Issues in Ecology, 2011. 2011.

Davidson, E.: Pulses of nitric oxide and nitrous oxide flux following wetting of dry soil: an assessment of probable sources and importance relative to annual fluxes, Ecol. Bull., 42, 149–155, 1992.

Del Grosso, S., Parton, W., Mosier, A., Ojima, D., Kulmala, A., and Phongpan, S.: General model for N2O and N2 gas emissions from soils due to dentrification, Global Biogeochemical Cycles, 14, 1045-1060, 2000.

Dinnes, D. L., Karlen, D. L., Jaynes, D. B., Kaspar, T. C., Hatfield, J. L., Colvin, T. S., and Cambardella, C. A.: Nitrogen management strategies to reduce nitrate leaching in tile-drained Midwestern soils, Agronomy journal, 94, 153-171, 2002.

Evans, S. E. and Burke, I. C.: Carbon and nitrogen decoupling under an 11-year drought in the shortgrass steppe, Ecosystems, 16, 20-33, 2013.

Firestone, M. K. and Davidson, E. A.: Microbiological basis of NO and N2O production and consumption in soil, Exchange of trace gases between terrestrial ecosystems and the atmosphere, 47, 7-21, 1989.

Frink, C. R., Waggoner, P. E., and Ausubel, J. H.: Nitrogen fertilizer: retrospect and prospect, Proceedings of the National Academy of Sciences, 96, 1175-1180, 1999.

Gaillard, R. K., Jones, C. D., Ingraham, P., Collier, S., Izaurralde, R. C., Jokela, W., Osterholz, W., Salas, W., Vadas, P., and Ruark, M.: Underestimation of N2O emissions in a comparison of the DayCent, DNDC, and EPIC models, Ecological Applications, 2017. 2017.

Geddes, J. A., Heald, C. L., Silva, S. J., and Martin, R. V.: Land cover change impacts on atmospheric chemistry: simulating projected large-scale tree mortality in the United States, Atmospheric Chemistry and Physics, 16, 2323-2340, 2016.

Gödde, M. and Conrad, R.: Influence of soil properties on the turnover of nitric oxide and nitrous oxide by nitrification and denitrification at constant temperature and moisture, Biology and Fertility of Soils, 32, 120-128, 2000.

Gollehon, N. R., Caswell, M., Ribaudo, M., Kellogg, R. L., Lander, C., and Letson, D.: Confined animal production and manure nutrients, United States Department of Agriculture, Economic Research Service, 2001.

Griffis, T. J., Chen, Z., Baker, J. M., Wood, J. D., Millet, D. B., Lee, X., Venterea, R. T., and Turner, P. A.: Nitrous oxide emissions are enhanced in a warmer and wetter world, Proceedings of the National Academy of Sciences, 114, 12081-12085, 2017.

Heil, J., Vereecken, H., and Brüggemann, N.: A review of chemical reactions of nitrification intermediates and their role in nitrogen cycling and nitrogen trace gas formation in soil, European journal of soil science, 67, 23-39, 2016.

Hickman, J. E., Wu, S., Mickley, L. J., and Lerdau, M. T.: Kudzu (Pueraria montana) invasion doubles emissions of nitric oxide and increases ozone pollution, Proceedings of the National Academy of Sciences, 107, 10115-10119, 2010. Holmes, N. S.: A review of particle formation events and growth in the atmosphere in the various environments and discussion of mechanistic implications, Atmospheric Environment, 41, 2183-2201, 2007.

Homyak, P. M. and Sickman, J. O.: Influence of soil moisture on the seasonality of nitric oxide emissions from chaparral soils, Sierra Nevada, California, USA, Journal of arid environments, 103, 46-52, 2014.

Homyak, P. M., Blankinship, J. C., Marchus, K., Lucero, D. M., Sickman, J. O., and Schimel, J. P.: Aridity and plant uptake interact to make dryland soils hotspots for nitric oxide (NO) emissions, Proceedings of the National Academy of Sciences, 113, E2608-E2616, 2016.

Houlton, B., Morford, S., and Dahlgren, R.: Convergent evidence for widespread rock nitrogen sources in Earth's surface environment, Science, 360, 58-62, 2018.

Hudman, R. C., Moore, N. E., Mebust, A. K., Martin, R. V., Russell, A. R., Valin, L. C., and Cohen, R. C.: Steps towards a mechanistic model of global soil nitric oxide emissions: implementation and space based-constraints, Atmos. Chem. Phys., 12, 7779– 7795, doi:10.5194/acp-12-7779-2012, 2012.

~~IPCC: Climate Change 2007: Impacts, Adaptation and Vulnerability, Contribution of Working Group II to the Fourth Assessment Report of the Intergovernmental Panel on Climate Change, edited by: Parry, M. L., Canziani, O. F., Palutikof, J. P., van der Linden, P. J., and Hanson, C. E., Cambridge University Press, Cambridge, UK, 976 pp., 2007.~~

Hutchinson, G. and Brams, E.: NO versus N2O emissions from an NH4+-amended Bermuda grass pasture, Journal of Geophysical Research: Atmospheres, 97, 9889-9896, 1992.

IPCC: Climate Change 20~~07~~13: The Physical Science Basis~~Impacts, Adaptation and Vulnerability, Contribution of~~ Working Group I~~I~~ Contribution to the ~~Fourth~~Fifth Assessment Report of the Intergovernmental Panel on Climate Change, edited by: ~~Parry, M. L., Canziani, O. F., Palutikof, J. P., van der Linden, P. J., and Hanson, C. E.~~T.F. Stocker et al., Cambridge University Press, Cambridge, UK, ~~976 pp.,~~ 2013~~07.~~

-Izaurralde, R. C., McGill, W. B., Williams, J. R., Jones, C. D., Link, R. P., Manowitz, D. H., Schwab, D. E., Zhang, X., Robertson, G. P., and Millar, N.: Simulating microbial denitrification with EPIC: Model description and evaluation, Ecological modelling, 359, 349-362, 2017.

Izaurralde, R. C., McGill, W. B., and Williams, J.: Development and application of the EPIC model for carbon cycle, greenhouse gas mitigation, and biofuel studies. In: Managing Agricultural Greenhouse Gases, Elsevier, 2012.

Izaurralde, R., Williams, J. R., Mcgill, W. B., Rosenberg, N. J., and Jakas, M. Q.: Simulating soil C dynamics with EPIC: Model description and testing against long-term data, Ecological Modelling, 192, 362-384, 2006.

Jaeglé, L., Martin, R. V., Chance, K., Steinberger, L., Kurosu, T. P., Jacob, D. J., Modi, A. I., Yoboué, V., Sigha-Nkamdjou, L., and Galy-Lacaux, C.: Satellite mapping of rain-induced nitric oxide emissions from soils, J. Geophys. Res.-Atmos., 109, D21310, doi:10.1029/2004JD004787, 2004.

Jaeglé, L., Steinberger, L., Martin, R. V., and Chance, K.: Global partitioning of NO x sources using satellite observations: Relative roles of fossil fuel combustion, biomass burning and soil emissions, Faraday Discussions, 130, 407-423, 2005.

Kampa, M. and Castanas, E.: Human health effects of air pollution, Environmental pollution, 151, 362-367, 2008.

Kellogg, R. L., Lander, C. H., Moffitt, D. C., and Gollehon, N.: Manure nutrients relative to the capacity of cropland and pastureland to assimilate nutrients: Spatial and temporal trends for the United States, Proceedings of the Water Environment Federation, 2000, 18-157, 2000.

Kesik, M., Blagodatsky, S., Papen, H., and Butterbach-Bahl, K.: Effect of pH, temperature and substrate on N2O, NO and CO2 production by Alcaligenes faecalis p, Journal of applied microbiology, 101, 655-667, 2006.

Kim, H. C., Lee, P., Judd, L., Pan, L., and Lefer, B.: OMI NO 2 column densities over North American urban cities: the effect of satellite footprint resolution, Geoscientific Model Development, 9, 2016.

Kottek, M., Grieser, J., Beck, C., Rudolf, B., and Rubel, F.: World Map of the Köppen-Geiger climate classification updated. *Meteorologische Zeitshrift*, 15, 259-263. DOI: 10.1127/0941-2948/2006/0130, 2006.

Kwok, R., Napelenok, S., and Baker, K.: Implementation and evaluation of PM2. 5 source contribution analysis in a photochemical model, Atmospheric environment, 80, 398-407, 2013.

Lamsal, L., Krotkov, N., Celarier, E., Swartz, W., Pickering, K., Bucsela, E., Gleason, J., Martin, R., Philip, S., and Irie, H.: Evaluation of OMI operational standard NO 2 column retrievals using in situ and surface-based NO 2 observations, Atmospheric Chemistry and Physics, 14, 11587-11609, 2014.

Laville, P., Lehuger, S., Loubet, B., Chaumartin, F., and Cellier, P.: Effect of management, climate and soil conditions on N2O and NO emissions from an arable crop rotation using high temporal resolution measurements, Agricultural and Forest Meteorology, 151, 228-240, 2011.

Leitner, S., Homyak, P. M., Blankinship, J. C., Eberwein, J., Jenerette, G. D., Zechmeister-Boltenstern, S., and Schimel, J. P.: Linking NO and N 2 O emission pulses with the mobilization of mineral and organic N upon rewetting dry soils, Soil Biology and Biochemistry, 115, 461-466, 2017.

Li, Y., Schichtel, B. A., Walker, J. T., Schwede, D. B., Chen, X., Lehmann, C. M., Puchalski, M. A., Gay, D. A., and Collett, J. L.: Increasing importance of deposition of reduced nitrogen in the United States, Proceedings of the National Academy of Sciences, 113, 5874-5879, 2016.

Liu, B., Mørkved, P. T., Frostegård, Å., and Bakken, L. R.: Denitrification gene pools, transcription and kinetics of NO, N2O and N2 production as affected by soil pH, FEMS microbiology ecology, 72, 407-417, 2010.

Liu, X., Ju, X., Zhang, Y., He, C., Kopsch, J., and Fusuo, Z.: Nitrogen deposition in agroecosystems in the Beijing area, Agriculture, ecosystems & environment, 113, 370-377, 2006.

Lu, C. and Tian, H.: Global nitrogen and phosphorus fertilizer use for agriculture production in the past half century: shifted hot spots and nutrient imbalance, Earth System Science Data, 9, 181, 2017.

Ludwig, J., Meixner, F., Vogel, B., and Förstner, J.: Soil-air exchange of nitric oxide: an overview of processes, environmental factors, and modeling studies, Biogeochemistry, 52, 225–257, doi:10.1023/A:1006424330555, 2001.

Machefert, S., Dise, N., Goulding, K., and Whitehead, P.: Nitrous oxide emission from a range of land uses across Europe, Hydrology and Earth System Sciences Discussions, 6, 325-338, 2002.

Maljanen, M., Yli-Pirilä, P., Hytönen, J., Joutsensaari, J., and Martikainen, P. J.: Acidic northern soils as sources of atmospheric nitrous acid (HONO), Soil Biology and Biochemistry, 67, 94-97, 2013.

Malm, W. C., Sisler, J. F., Huffman, D., Eldred, R. A., and Cahill, T. A.: Spatial and seasonal trends in particle concentration and optical extinction in the United States, Journal of Geophysical Research: Atmospheres, 99, 1347-1370, 1994.

Mamtimin, B., Meixner, F. X., Behrendt, T., Badawy, M., and Wagner, T.: The contribution of soil biogenic NO and HONO emissions from a managed hyperarid ecosystem to the regional NO x emissions during growing season, Atmospheric Chemistry and Physics, 16, 10175-10194, 2016.

Manzoni, S. and Porporato, A.: Soil carbon and nitrogen mineralization: theory and models across scales, Soil Biology and Biochemistry, 41, 1355-1379, 2009.

Martin, R. E., Scholes, M., Mosier, A., Ojima, D., Holland, E., and Parton, W.: Controls on annual emissions of nitric oxide from soils of the Colorado shortgrass steppe, Global Biogeochemical Cycles, 12, 81-91, 1998.

Medinets, S., Skiba, U., Rennenberg, H., and Butterbach-Bahl, K.: A review of soil NO transformation: Associated processes and possible physiological significance on organisms, Soil Biology and Biochemistry, 80, 92-117, 2015.

Moldrup, P., Olesen, T., Yoshikawa, S., Komatsu, T., and Rolston, D. E.: Three-porosity model for predicting the gas diffusion coefficient in undisturbed soil, Soil Science Society of America Journal, 68, 750-759, 2004.

Montes, F., Meinen, R., Dell, C., Rotz, A., Hristov, A., Oh, J., Waghorn, G., Gerber, P., Henderson, B., and Makkar, H.: SPECIAL TOPICS—mitigation of methane and nitrous oxide emissions from animal operations: II. A review of manure management mitigation options, Journal of Animal Science, 91, 5070-5094, 2013.

Necpálová, M., Anex, R. P., Fienen, M. N., Del Grosso, S. J., Castellano, M. J., Sawyer, J. E., Iqbal, J., Pantoja, J. L., and Barker, D. W.: Understanding the DayCent model, Environmental Modelling & Software, 66, 110-130, 2015.

Neira, M.: The 2014 WHO conference on health and climate. SciELO Public Health, 2014.

Oikawa, P., Ge, C., Wang, J., Eberwein, J., Liang, L., Allsman, L., Grantz, D., and Jenerette, G.: Unusually high soil nitrogen oxide emissions influence air quality in a high-temperature agricultural region, Nature communications, 6, 8753, 2015.

Otte, T. L. and Pleim, J. E.: The Meteorology-Chemistry Interface Processor (MCIP) for the CMAQ modeling system: updates through MCIPv3.4.1, Geosci. Model Dev., 3, 243-256, doi:10.5194/gmd-3-243-2010, 2010.

Parrish, D., Williams, E., Fahey, D., Liu, S., and Fehsenfeld, F.: Measurement of nitrogen oxide fluxes from soils: Intercomparison of enclosure and gradient measurement techniques, Journal of Geophysical Research: Atmospheres, 92, 2165-2171, 1987.

Parton, W. J., Holland, E. A., Del Grosso, S. J., Hartman, M. D., Martin, R. E., Mosier, A. R., Ojima, D. S., and Schimel, D. S.: Generalized model for NO_x and N_2O emissions from soils, J. Geophys. Res.-Atmos., 106, 17403–17419, doi:10.1029/2001JD900101, 2001.

Parton, W. J., Ojima, D. S., Cole, C. V., and Schimel, D. S.: A general model for soil organic matter dynamics: sensitivity to litter chemistry, texture and management, Quantitative modeling of soil forming processes, 1994. 147-167, 1994.

Pilegaard, K., Skiba, U., Ambus, P., Beier, C., Brüggemann, N., Butterbach-Bahl, K., Dick, J., Dorsey, J., Duyzer, J., and Gallagher, M.: Nitrogen load and forest type determine the soil emission of nitrogen oxides (NO and N 2 O), Biogeosciences Discussions, 3, 837-869, 2006.

Pilegaard, K.: Processes regulating nitric oxide emissions from soils, Philosophical Transactions of the Royal Society B: Biological Sciences, 368, 20130126, 2013.Pleim, J.E. and Xiu, A.: Development of a land surface model. Part II: Data assimilation. Journal of Applied Meteorology, 42(12), pp.1811-1822, 2003.

Pope, C. A., Burnett, R. T., Krewski, D., Jerrett, M., Shi, Y., Calle, E. E., and Thun, M. J.: Cardiovascular mortality and exposure to airborne fine particulate matter and cigarette smoke: shape of the exposure-response relationship, Circulation, 120, 941-948, 2009.

Potter, P., Navin, R., Elena M. B., and Simon D. D.: Characterizing the spatial patterns of global fertilizer application and manure production. *Earth Interactions*, 14, no. 2: 1-22, 2010.

Pouliot, G. and Pierce, T.: Integration of the Model of Emissions of Gases and Aerosols from Nature (MEGAN) into the CMAQ Modeling System, 2009, 14-17.

Pouliot, G.: A tale of two models: a comparison of the Biogenic Emission Inventory System (BEIS3. 14) and Model of Emissions of Gases and Aerosols from Nature (MEGAN 2.04), 2008.

Rasool, Q.Z., R. Zhang, B. Lash, D.S. Cohan, E. Cooter, J. Bash, L.N. Lamsal. Enhanced representation of soil NO emissions in the Community Multi-scale Air Quality (CMAQ) model version 5.0.2. *Geoscientific Model Development*, 9, 3177-3197, 2016.

Rasool, Q.Z., Bash, J.O., and Cohan, D.S.: Mechanistic representation of soil nitrogen emissions in CMAQ version 5.1, ORNL DAAC, Oak Ridge, Tennessee, USA, https://doi.org/10.3334/ORNLDAAC/1661, 2018.

Redding, M., Shorten, P., Lewis, R., Pratt, C., Paungfoo-Lonhienne, C., and Hill, J.: Soil N availability, rather than N deposition, controls indirect N2O emissions, Soil Biology and Biochemistry, 95, 288-298, 2016.

Ribaudo, M., Key, N., and Sneeringer, S.: The potential role for a nitrogen compliance policy in mitigating Gulf hypoxia, Applied Economic Perspectives and Policy, 39, 458-478, 2016.

Ribaudo, M., Livingston, M., and Williamson, J.: Nitrogen management on us corn acres, 2001-10, United States Department of Agriculture, Economic Research Service, 2012.

Ribaudo, M., Gollehon, N., and Agapoff, J.: Land application of manure by animal feeding operations: Is more land needed?, Journal of Soil and Water Conservation, 58, 30-38, 2003.

Robertson, G. P. and Groffman, P.: Nitrogen transformations. In: Soil Microbiology, Ecology and Biochemistry (Third Edition), Elsevier, 2007.

Schimel, J. P. and Weintraub, M. N.: The implications of exoenzyme activity on microbial carbon and nitrogen limitation in soil: a theoretical model, Soil Biology and Biochemistry, 35, 549-563, 2003.

Schindlbacher, A., Zechmeister-Boltenstern, S., and Butterbach-Bahl, K.: Effects of soil moisture and temperature on NO, NO2, and N2O emissions from European forest soils, Journal of Geophysical Research: Atmospheres, 109, 2004.

Scholes, M., Martin, R., Scholes, R., Parsons, D., and Winstead, E.: NO and N_2O emissions from savanna soils following the first simulated rains of the season, Nutr. Cycl. Agroecosys., 48, 115–122, doi:10.1023/A:1009781420199, 1997.

Seinfeld, John H., and Spyros N. Pandis. Atmospheric chemistry and physics: from air pollution to climate change. John Wiley & Sons, 2012.

Simon, H., Reff, A., Wells, B., Xing, J., and Frank, N.: Ozone trends across the United States over a period of decreasing NOx and VOC emissions, Environmental science & technology, 49, 186-195, 2014.

Skamarock, W. C., Klemp, J. B., Dudhia, J., Gill, D. O., Barker, D. M., Duda, M. G., Huang, X., Wang, W., and Powers, J. G.: A description of the advanced research WRF version 3, NCAR Tech. Note, NCAR/TN-475+STR, 8 pp., Natl. Cent. for Atmos. Res., Boulder, Colo., 2008 (available at: http://www.mmm.ucar.edu/wrf/users/docs/arw_v3.pdf)

Stehfest, E., & Bouwman, L.: N_2O and NO emission from agricultural fields and soils under natural vegetation: summarizing available measurement data and modeling of global annual emissions. Nutrient Cycling in Agroecosystems, 74(3), 207-228.doi: 10.1007/s10705-006-9000-7, 2006.

Steinkamp, J., & Lawrence, M. G.: Improvement and evaluation of simulated global biogenic soil NO emissions in an AC-GCM. Atmospheric Chemistry and Physics, 11(12), 6063–6082. doi:10.5194/acp-11-6063-2011, 2011.

Strode, S. A., Rodriguez, J. M., Logan, J. A., Cooper, O. R., Witte, J. C., Lamsal, L. N., Damon, M., Van Aartsen, B., Steenrod, S. D., and Strahan, S. E.: Trends and variability in surface ozone over the United States, J. Geophys. Res. Atmos., 120, 9020–9042, doi:10.1002/2014JD022784, 2015.

Su, H., Cheng, Y., Oswald, R., Behrendt, T., Trebs, I., Meixner, F. X., Andreae, M. O., Cheng, P., Zhang, Y., and Pöschl, U.: Soil nitrite as a source of atmospheric HONO and OH radicals, Science, 333, 1616-1618, 2011.

Tilman, D., Fargione, J., Wolff, B., D'antonio, C., Dobson, A., Howarth, R., Schindler, D., Schlesinger, W. H., Simberloff, D., and Swackhamer, D.: Forecasting agriculturally driven global environmental change, Science, 292, 281-284, 2001.

Townsend, A. R., Howarth, R. W., Bazzaz, F. A., Booth, M. S., Cleveland, C. C., Collinge, S. K., Dobson, A. P., Epstein, P. R., Holland, E. A., and Keeney, D. R.: Human health effects of a changing global nitrogen cycle, Frontiers in Ecology and the Environment, 1, 240-246, 2003.

Venterea, R. T. and Rolston, D. E.: Mechanisms and kinetics of nitric and nitrous oxide production during nitrification in agricultural soil, Global Change Biology, 6, 303-316, 2000.

Vinken, G. C. M., Boersma, K. F., Maasakkers, J. D., Adon, M., & Martin, R. V. (2014). Worldwide biogenic soil NO_x emissions inferred from OMI NO_2 observations. Atmospheric Chemistry and Physics, 14(18), 10363–10381. doi:10.5194/acp-14-10363-2014.

Wade, T., Claassen, R. L., and Wallander, S.: Conservation-practice adoption rates vary widely by crop and region, United States Department of Agriculture, Economic Research Service, 2015.

Wang, C., Houlton, B. Z., Dai, W., and Bai, E.: Growth in the global N2 sink attributed to N fertilizer inputs over 1860 to 2000, Science of the Total Environment, 574, 1044-1053, 2017.

Wang, L., Xu, J., Yang, J., Zhao, X., Wei, W., Cheng, D., Pan, X., and Su, J.: Understanding haze pollution over the southern Hebei area of China using the CMAQ model, Atmospheric Environment, 56, 69-79, 2012.

Wang, Y., Logan, J. A., and Jacob, D. J.: Global simulation of tropospheric O3-NO x-hydrocarbon chemistry: 2. Model evaluation and global ozone budget, Journal of Geophysical Research: Atmospheres (1984–2012), 103, 10727-10755, 1998.

Wang, Y., Zhang, Q. Q., He, K., Zhang, Q., and Chai, L.: Sulfate-nitrate-ammonium aerosols over China: response to 2000–2015 emission changes of sulfur dioxide, nitrogen oxides, and ammonia, Atmos. Chem. Phys., 13, 2635-2652, doi:10.5194/acp-13-2635-2013, 2013.

Weier, K., Doran, J., Power, J., and Walters, D.: Denitrification and the dinitrogen/nitrous oxide ratio as affected by soil water, available carbon, and nitrate, Soil Science Society of America Journal, 57, 66-72, 1993.

Williams, E. and Fehsenfeld, F.: Measurement of soil nitrogen oxide emissions at three North American ecosystems, Journal of Geophysical Research: Atmospheres, 96, 1033-1042, 1991.

Williams, E. J., A. Guenther, F. C. Fehsenfeld, An inventory of nitric oxide emissions from soils in the United States, J. Geophys. Res., 97, 7511–7519, 1992.

Williams, E. J., Parrish, D. D., Buhr, M. P., Fehsenfeld, F. C., and Fall, R.: Measurement of soil NO_x emissions in central Pennsylvania, J. Geophys. Res.-Atmos., 93, 9539–9546, doi:10.1029/JD093iD08p09539, 1988.

Williams, J., Izaurralde, R., and Steglich, E.: Agricultural policy/environmental extender model, Theoretical Documentation, Version, 604, 2008-2017, 2008.

Xu, X., Thornton, P. E., and Post, W. M.: A global analysis of soil microbial biomass carbon, nitrogen and phosphorus in terrestrial ecosystems, Global Ecology and Biogeography, 22, 737-749, 2013.

Xu, X., Thornton, P., and POTAPOV, P.: A Compilation of Global Soil Microbial Biomass Carbon, Nitrogen, and Phosphorus Data, ORNL DAAC, 2015. 2015.

Yienger, J. and Levy, H.: Empirical model of global soil-biogenic NO_x emissions, Journal of Geophysical Research: Atmospheres, 100, 11447-11464, 1995.

Zhu, L., Henze, D., Bash, J., Jeong, G.-R., Cady-Pereira, K., Shephard, M., Luo, M., Paulot, F., and Capps, S.: Global evaluation of ammonia bidirectional exchange and livestock diurnal variation schemes, Atmos. Chem. Phys., 15, 12823–12843, doi:10.5194/acp-15-12823-2015, 2015.

a)

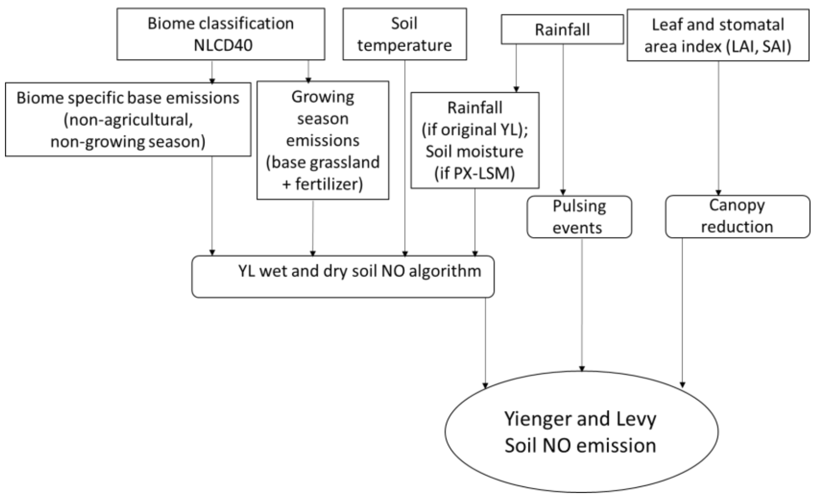
Biome classification
NLCD40
Soil
temperature
Rainfall
Leaf and stomatal
area index (LAI, SAI)
Biome specific base emissions
(non-agricultural,
non-growing season)
Growing
season
emissions
(base grassland
+ fertilizer)
Rainfall
(if original YL);
Soil moisture
(if PX-LSM)
Pulsing
events
Canopy
reduction
YL wet and dry soil NO algorithm
Yienger and Levy
Soil NO emission

b)

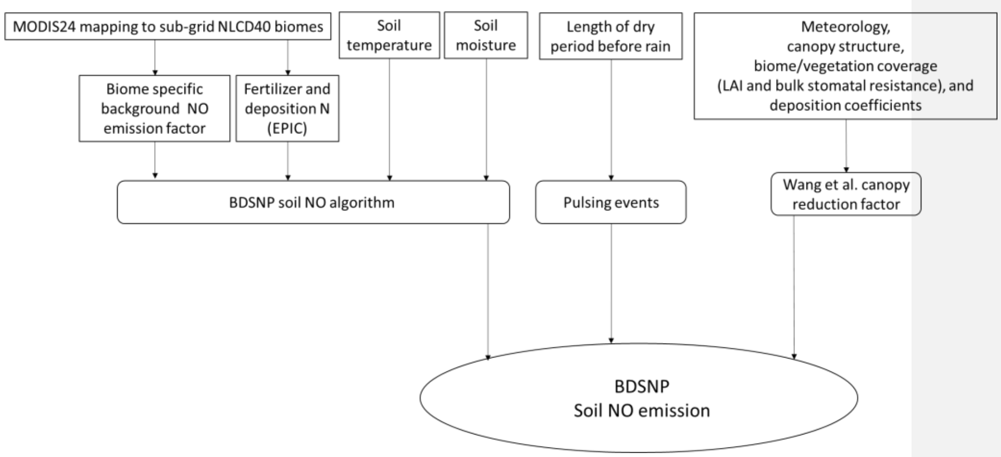
MODIS24 mapping to sub-grid NLCD40 biomes
Soil
temperature
Soil
moisture
Length of dry
period before rain
Meteorology,
canopy structure,
biome/vegetation coverage
(LAI and bulk stomatal resistance), and
deposition coefficients
Biome specific
background NO
emission factor
Fertilizer and
deposition N
(EPIC)
BDSNP soil NO algorithm
Pulsing events
Wang et al. canopy
reduction factor
BDSNP
Soil NO emission

c)

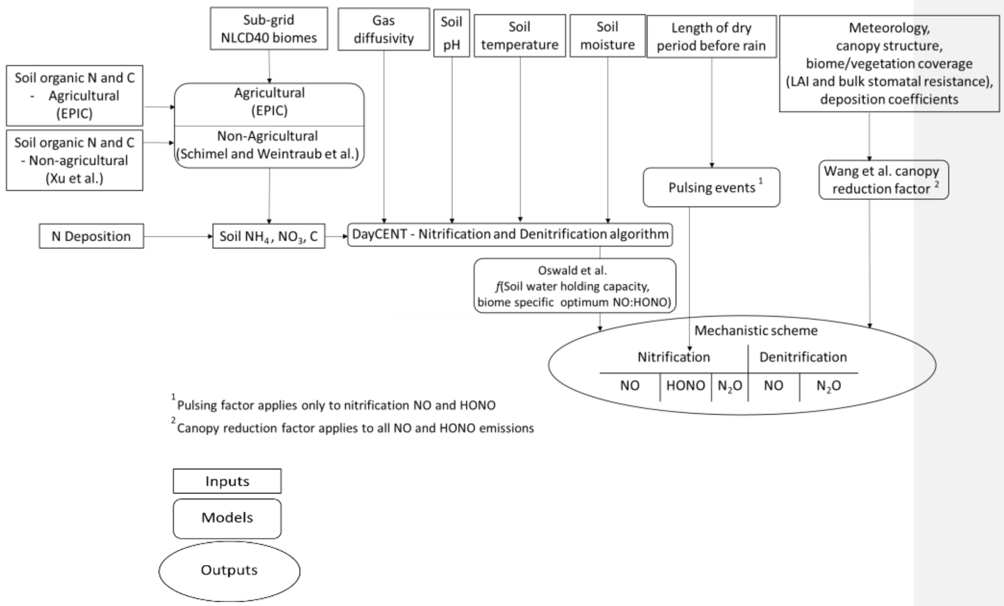

Figure 1 Flowchart of the a) Yienger and Levy, 1995 (YL), b) Berkley Dalhousie Soil NO_x Parametrization (BDSNP), and c) Mechanistic schemes for soil Nitrogen (N) emissions as implemented in CMAQ.

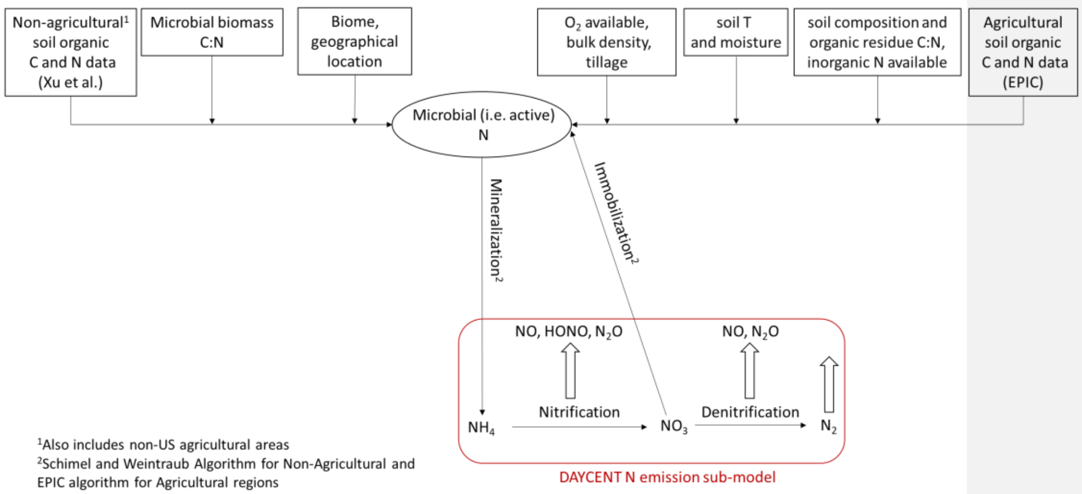

Figure 2 Schematic for N transformation to estimate soil pools of ammonium (NH_4) and nitrate (NO_3) and resultant nitrification and denitrification N emissions in the mechanistic model.

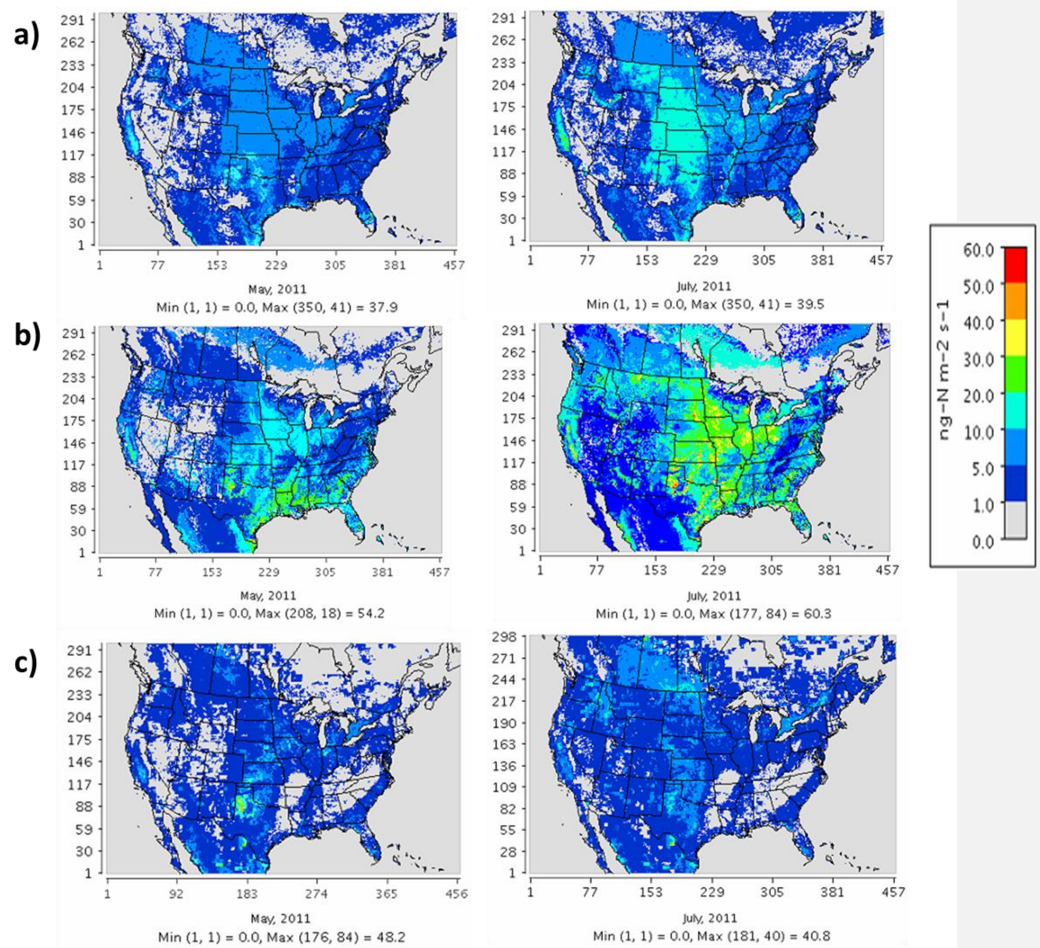

Figure 3 Soil N oxide emissions on a monthly average basis for May (left) and July (right) 2011 for: a) YL scheme (NO), b) Parameterized BDSNP scheme (NO) and c) Mechanistic scheme (NO + HONO).

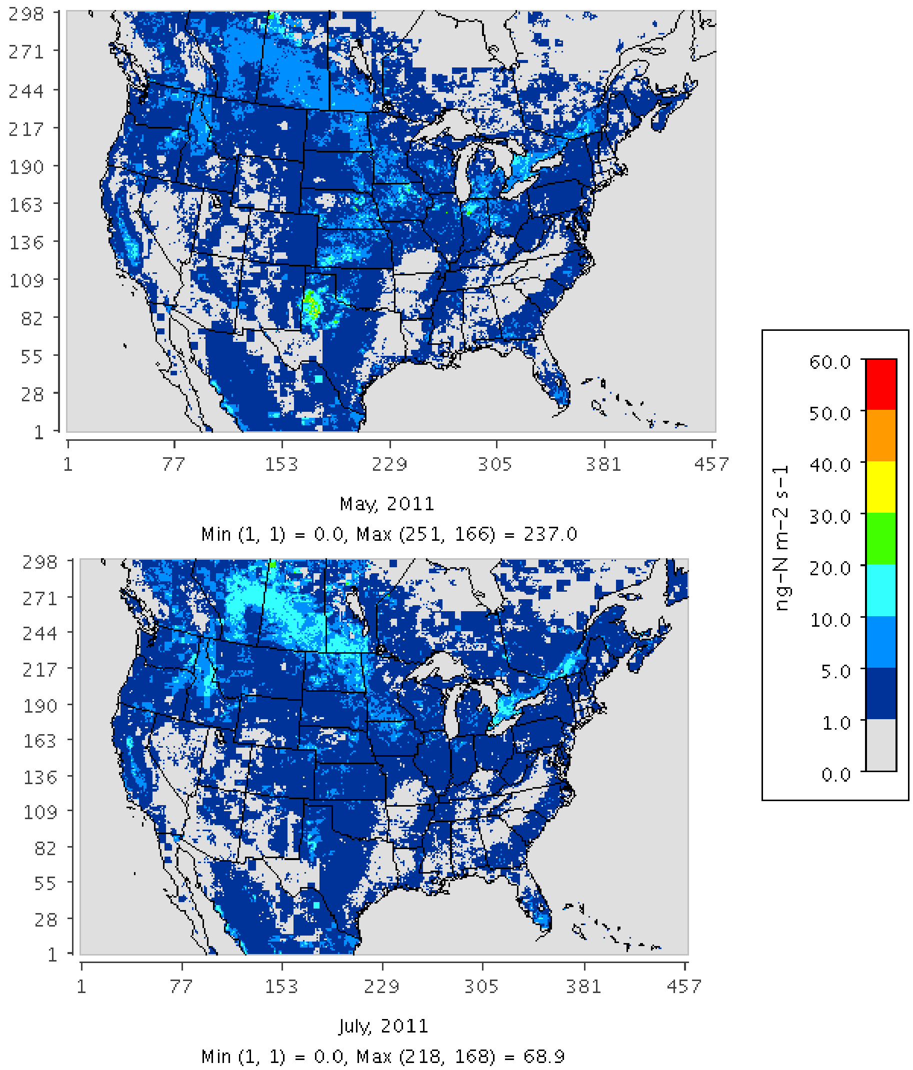

Figure 4 Soil N_2O emissions on a monthly average basis for May (top) and July (bottom) 2011 estimated from mechanistic scheme.

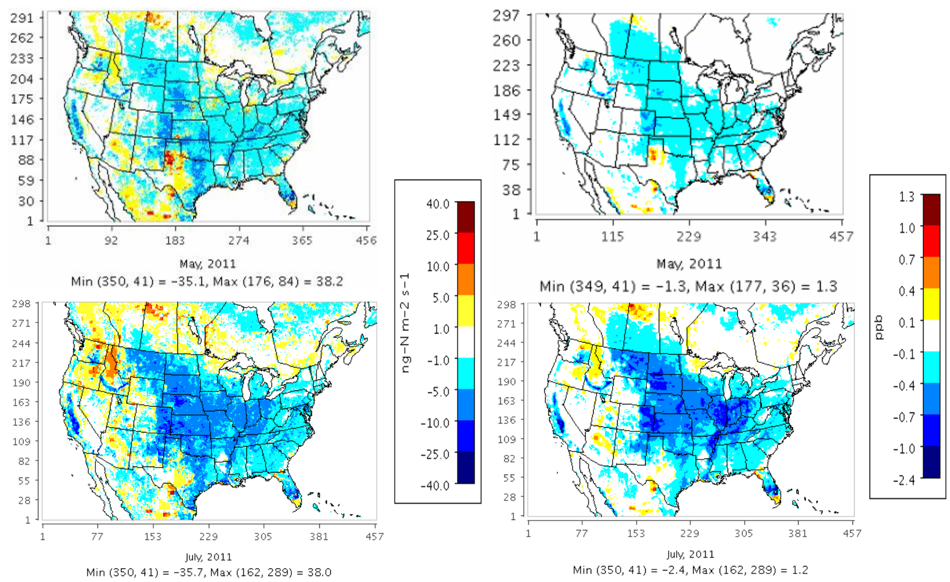

Figure 5 Total NO_x ($NO + NO_2$) concentration sensitivity (right) to changes in soil NO_x emissions (left) on a monthly average basis for May (top) and July (bottom) 2011, when switching from YL scheme (NO) to Mechanistic scheme (NO + HONO).

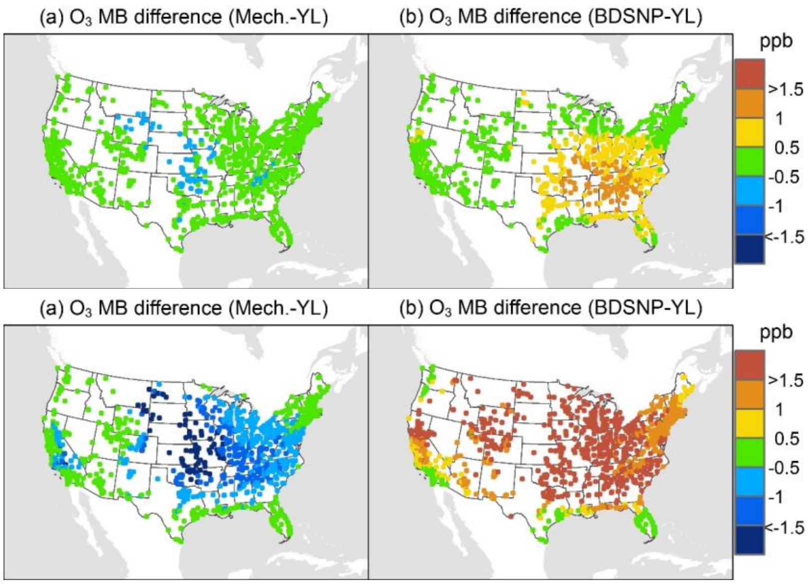

Figure 6 Change in average monthly mean bias (MB) of Community Multiscale Air Quality (CMAQ) model evaluated against EPA's Air Quality System (AQS) O_3 observations for May (top) and July (bottom) 2011 when switching to Mechanistic (a) or BDSNP (b) scheme from YL.

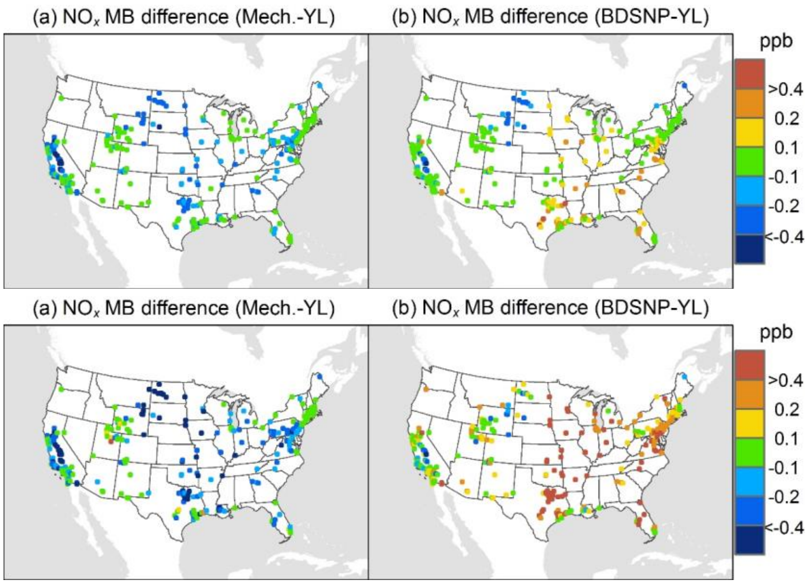

Figure 7 Change in average monthly MB of CMAQ evaluated against EPA's AQS NO$_x$ observations for May (top) and July (bottom) 2011 when switching to Mechanistic (a) or BDSNP (b) scheme from YL.

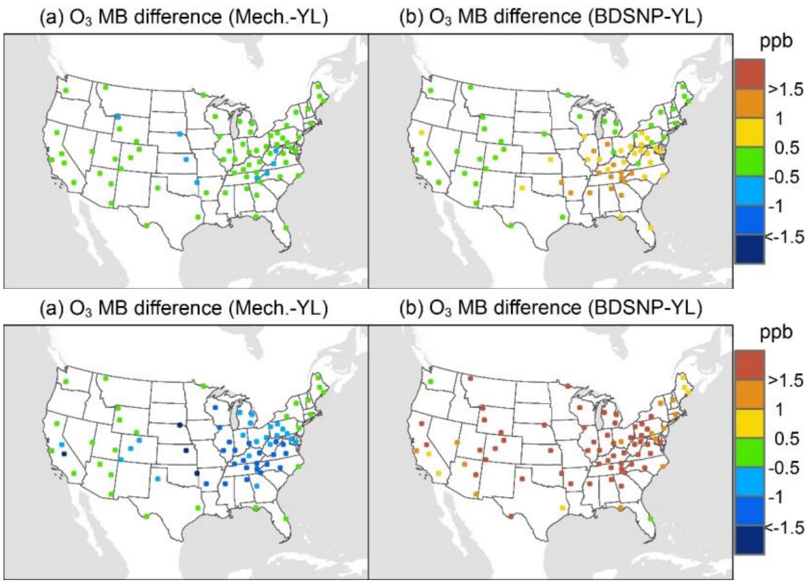

Figure 8 Change in average monthly MB of CMAQ evaluated against EPA's Clean Air Status and Trends Network (CASTNET) O_3 observations for May (top) and July (bottom) 2011 when switching to Mechanistic (a) or BDSNP (b) scheme from YL.

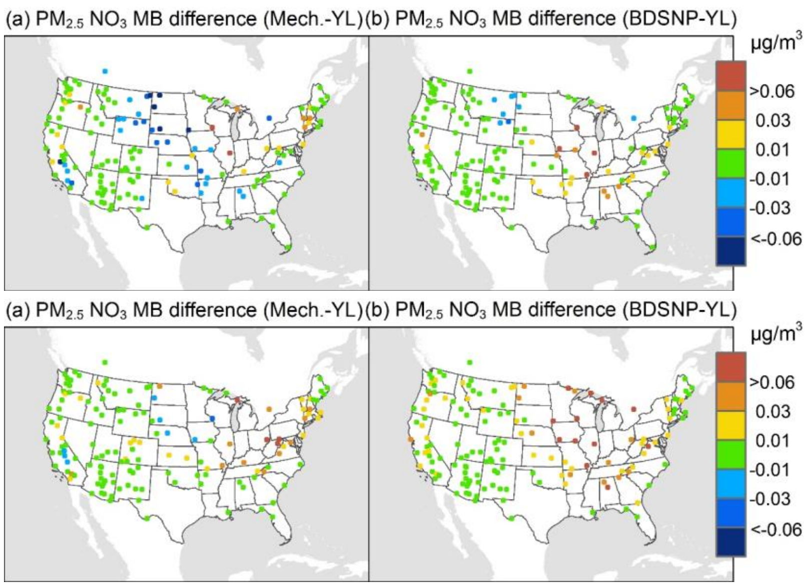

Figure 9 Change in average monthly MB of CMAQ evaluated against Interagency Monitoring of Protected Visual Environments (IMPROVE) $PM_{2.5}$ NO_3 observations for May (top) and July (bottom) 2011 when switching to Mechanistic (a) or BDSNP (b) scheme from YL.

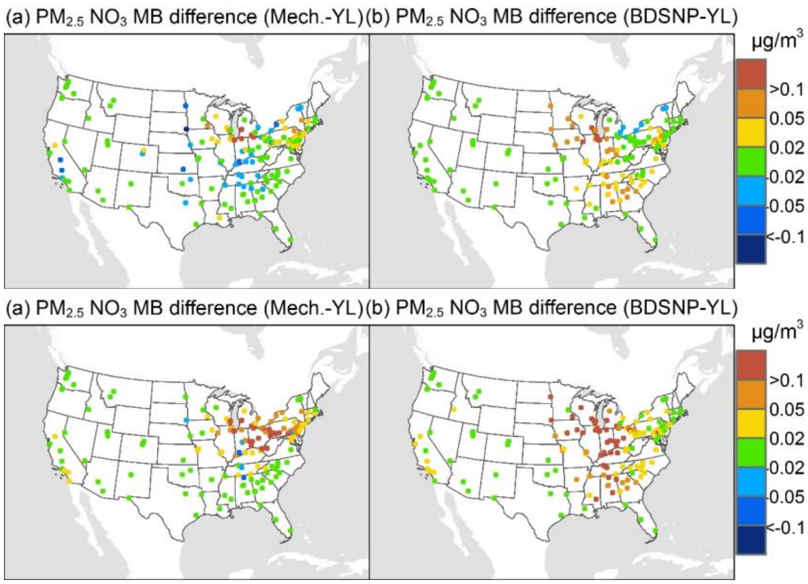

Figure 10 Change in average monthly MB of CMAQ evaluated against Chemical Speciation Network (CSN) $PM_{2.5}$ NO_3 observations for May (top) and July (bottom) 2011 when switching to Mechanistic (a) or BDSNP (b) scheme from YL.

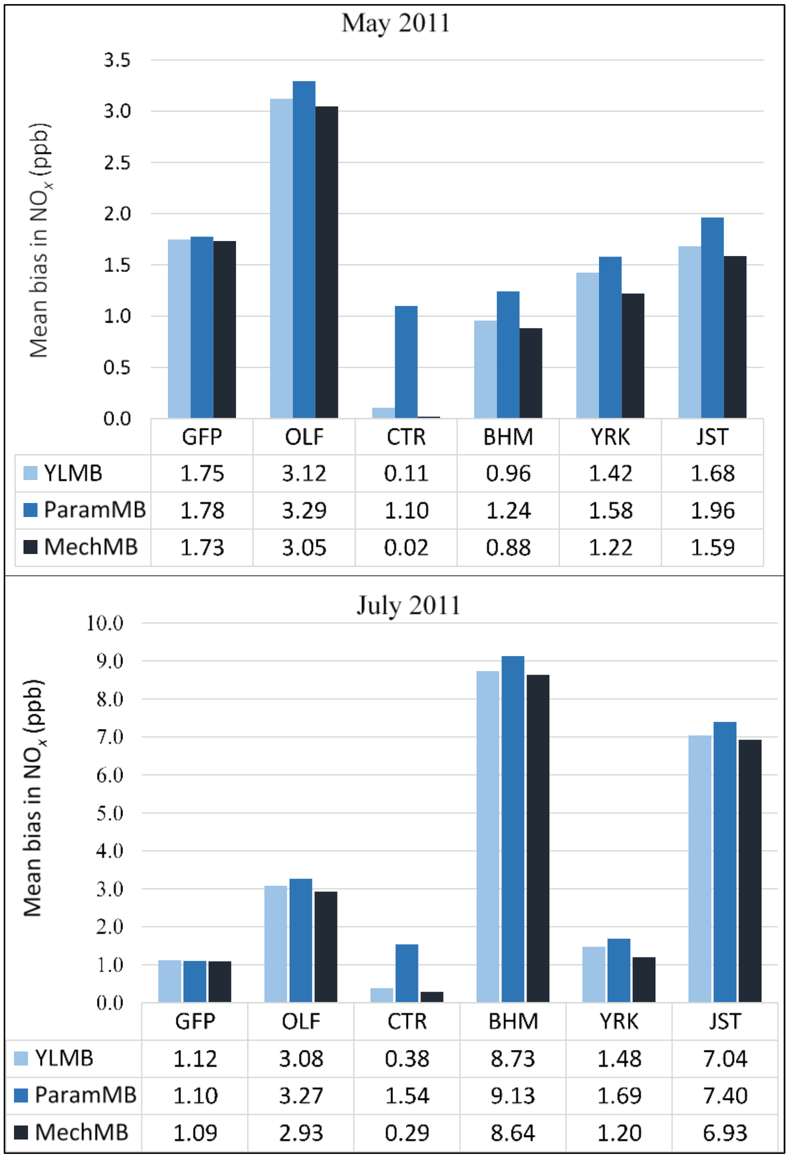

Figure 11 Comparison of average monthly (May and July 2011) MB for CMAQ NO_x with (a) YL (b) BDSNP parameterized and (c) Mechanistic schemes compared to South Eastern Aerosol Research and CHaracterization (SEARCH) NO_x observations in non-agricultural remote regions.

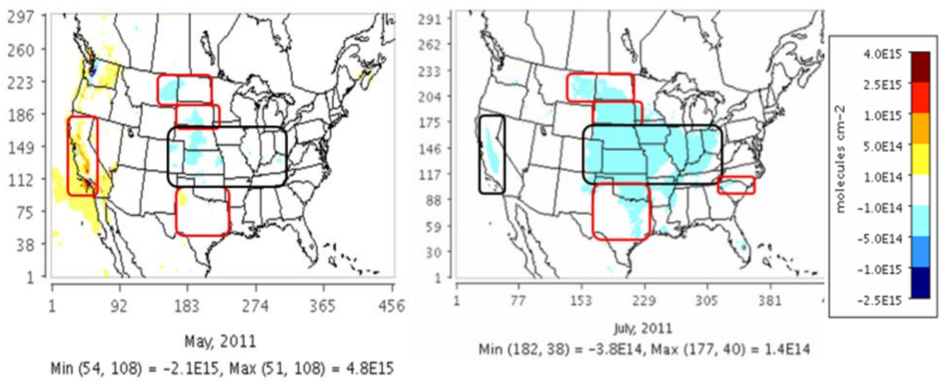

Figure 12 Impact of switching from YL scheme to Mechanistic scheme on CMAQ tropospheric NO_2 column density at NASA's Ozone Monitoring Instrument (OMI) overpass time (13:00-14:00 local time) on a monthly average (May and July 2011) basis.

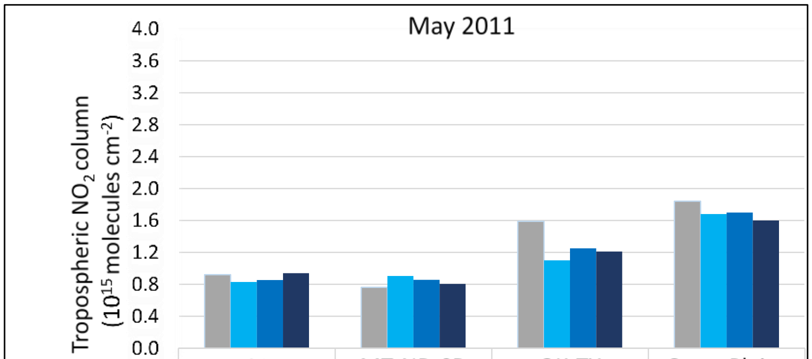

	CA	MT-ND-SD	OK-TX	Great Plains
OMI	0.92	0.76	1.59	1.84
YL	0.83	0.91	1.10	1.68
BDSNP	0.85	0.86	1.25	1.70
Mechanistic	0.94	0.81	1.21	1.60

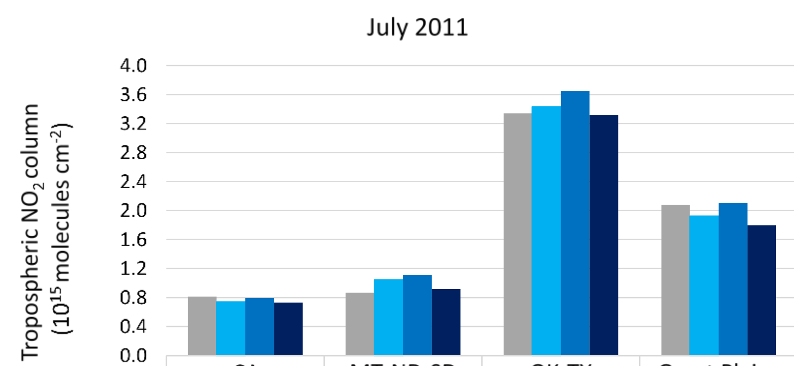

	CA	MT-ND-SD	OK-TX	Great Plains
OMI	0.81	0.87	3.34	2.08
YL	0.74	1.04	3.43	1.92
BDSNP	0.79	1.11	3.65	2.11
Mechanistic	0.73	0.92	3.32	1.80

Figure 13 Comparison of average monthly (May and July 2011) OMI NO_2 column densities with CMAQ tropospheric NO_2 column density using YL, BDSNP, and Mechanistic schemes. Regions are depicted in Figure 12.

Table 1: Comparison of approaches of the parametric and mechanistic soil N emissions models.

	YL Parametric Model	**BDSNP Parametric Model**	**Mechanistic Model**
Approach	Yienger and Levy equations for NO	Hudman et al. equations for NO	DayCENT sub-model representing nitrification, denitrification, and mineralization for NO, HONO, and N_2O
Species Emitted/Output	NO	NO	NO, HONO, NH_3, N_2O
Biome/Land use classification	CMAQ default NLCD40	Sub-grid biome classification; MODIS 24 mapped from NLCD40	Sub-grid biome classification from NLCD40
Soil N Data Source	Fertilizer N in growing season wet emission factor	EPIC (Fertilizer N + Deposition (wet and dry) N from CMAQ)	EPIC (Fertilizer N + Deposition (wet and dry) N from CMAQ); Xu et al. (2015) for non-agricultural soil
Agricultural biome	Biome specific NO emission factors	NO emissions derived from total EPIC N	EPIC C and N pools used in DayCENT scheme Nitrification NO, HONO and N_2O; Denitrification NO and N_2O
Nonagricultural biome	Biome specific NO emission factors	Biome specific NO emission factors	Schimel and Weintraub equations for N and C pools used in DayCENT to derive nitrification and denitrification emissions
Variables Considered	Soil T, rainfall, and biome type	Total soil N, soil T, soil moisture, rainfall, and biome type	Soil water content (irrigated and unirrigated), T, NH_4^+, NO_3^-, gas diffusivity, and labile C by soil layer
Pulsing	$f(precipitation)$	$f(l_{dry})$, with exponential decay with change in soil moisture	Same as BDSNP
CRF	$f(LAI, SAI)$	$f(LAI, Meterology, Biome)$	Same as BDSNP

Table 2 Modeling configuration used for the WRF-CMAQ simulations.

WRF/MCIP			
Version:	ARW V3.7	**Shortwave radiation:**	RRTMG Scheme
Horizontal resolution:	CONUS (12kmX12km)	**Surface layer physic:**	PX LSM
Vertical resolution:	35layer	**PBL scheme:**	ACM2
Boundary condition:	NARR 32km	**Microphysics:**	Morrison double-moment scheme
Initial condition:	NCEP-ADP	**Cumulus parameterization:**	Kain-Fritsch scheme
Longwave radiation:	Rapid Radiation Transfer Model Global (RRTMG) Scheme	**Assimilation:**	Analysis nudging above PBL for temperature, moisture and wind speed
BDSNP			
Horizontal resolution:	Same as WRF/MCIP	**Emission factor:**	Steinkamp and Lawrence (2011)
Soil Biome type:	Sub-grid biome fractions from WRFv3.7	**Fertilizer database:**	EPIC 2011 based from FEST-C v1.2
CMAQ			
Version:	5.1	**Anthropogenic emission:**	NEI 2011 v1
Horizontal resolution:	Same as WRF/MCIP	**Biogenic emission:**	BEIS v3.61 in-line
Initial condition:	Pleim-Xiu (MET) GEOS-Chem (CHEM)	**Boundary condition:**	Pleim-Xiu (MET) GEOS-Chem (CHEM)
Aerosol module:	AE6	**Gas-phase mechanism:**	CB-05
Simulation Case Arrangement (in-line with CMAQ)			
1. YL:	WRF/MCIP-CMAQ with standard YL soil NO scheme		
2. BDSNP (EPIC with new Biome):	WRF/MCIP-BDSNP-CMAQ with EPIC and new sub-grid biome fractions		
3. Mechanistic Scheme:	WRF/MCIP-Mechanistic soil N-CMAQ with EPIC (agricultural US) and Xu et al. (2015) (non-US agricultural and all non-agricultural in CONUS), new sub-grid biome fractions		
Simulation Time Period			
	May 1-31 and July 1-31, 2011 (10 day spin-up for each) for CMAQ simulation with **in-line YL, updated BDSNP and Mechanistic modules**		
Model Performance Evaluation			
USEPA Clean Air Status and Trends Network (CASTNET) and Air Quality System (AQS) data for ozone			
Interagency Monitoring of Protected Visual Environments (IMPROVE) and Chemical Speciation Network (CSN) (Malm et al., 1994) for $PM_{2.5}$ Nitrate			
AQS and South Eastern Aerosol Research and CHaracterization (SEARCH) for NO_x concentrations			
NASA's Ozone Monitoring Instrument (OMI) ~~NO_2~~ satellite retrieval product as derived in Lamsal et al., 2014 for tropospheric NO_2 column			

Table 3 NO emission rates (ng-N m^{-2} s^{-1}) observed in field studies in agricultural and grassland locations, and modeled by CMAQ with the three soil N schemes for May and July 2011. Observed and modeled values are from peak location/site within a range of values across sites.

Location (Study)	**Observed peak summertime soil NO**	**Mechanistic soil NO[b]**		**YL soil NO**		**BDSNP soil NO**	
		May 2011	**July 2011**	**May 2011**	**July 2011**	**May 2011**	**July 2011**
Iowa fertilized fields (Williams et al., 1992)	18.0	17.1	13.0	8.2	11.4	20.1	41.7
Montana fertilized fields[a] (Bertram et al., 2005)	12.0	7.8	14.2	7.1	12.9	9.8	42.3
South Dakota fertilized fields (Williams et al., 1991)	10.0	11.7	10.0	8.0	13.9	18.4	54.6
Texas grasses and fields (both fertilized) (Hutchinson and Brams, 1992)	43.0	52.5	45.0	15.0	15.9	54.1	60.3
Colorado natural grasslands (Parrish et al., 1987; Williams et al., 1991; Martin et al., 1998)	10.0	7.9	11.5	9.7	15.3	18.6	33.2

[a] Derived from SCIAMACHY NO_2 columns

[b] Mechanistic scheme estimates are NO + HONO emission rates

Table 4 Statistical performance of CMAQ modeled (with YL, updated BDSNP, and Mechanistic schemes) tropospheric NO_2 column for May 2011 with OMI NO_2 observations for sensitive sub-domains for CONUS.

	Domains	Correlation (r^2)			NMB (%)			NME (%)		
		YL	BDSNP	Mech.	YL	BDSNP	Mech.	YL	BDSNP	Mech.
May	**California**	0.86	0.86	0.85	-18.6	-17.0	-5.1	35.5	35.4	33.6
	OK-TX	0.19	0.30	0.30	-30.7	-21.7	-23.7	32.2	24.3	25.8
	MT-ND	0.35	0.34	0.34	+24.9	+13.4	+11.1	38.3	35.0	34.3
	SD	0.15	0.16	0.16	+13.4	+11.8	+0.8	27.5	28.6	25.2
	Great Plains	0.68	0.69	0.68	-11.0	-8.7	-14.7	27.8	26.8	29.5
	NC-SC-GA	0.65	0.65	0.65	-4.7	-1.3	-7.0	28.9	27.7	29.9
	CONUS	0.71	0.71	0.70	-10.9	-9.3	-10.6	38.2	37.3	38.6
July	**California**	0.78	0.78	0.79	-17.4	-11.5	-19.0	40.8	41.3	41.8
	OK-TX	0.79	0.79	0.79	+3.0	+9.3	-0.6	17.2	18.0	18.1
	MT-ND	0.44	0.40	0.43	28.5	41.6	13.0	31.6	42.9	23.5
	SD	0.25	0.16	0.18	15.5	18.8	0.6	20.1	22.8	16.7
	Great Plains	0.69	0.71	0.69	-16.8	-8.6	-22.8	25.4	20.4	30.0
	NC-SC-GA	0.55	0.54	0.55	25.4	31.1	20.9	30.0	33.3	28.8
	CONUS	0.74	0.75	0.72	-12.0	-5.9	-15.0	35.7	34.3	37.4

Appendix

Table A1 List of 24 MODIS soil biome based Cmic, Nmic and $HONO_f$ emission factors (%) derived from Xu et al. (2013) and Oswald et al. (2013)

ID	**MODIS land cover**	**Köppen main climate[c]**	**Cmic %**	**Nmic %**	**$HONO_f$ %**
1	Water	--	0	0	0
2	Permanent wetland	--	1.20	2.58	0
3	Snow and ice	--	0	0	0
4	Barren	D,E	5.02	5.72	48
5	Unclassified	--	0	0	0
6	Barren	A,B,C	5.02	5.72	48
7	Closed shrub land	--	1.43	2.33	35.5
8	Open shrub land	A,B,C	1.43	2.33	41
9	Open shrub land	D,E	1.43	2.33	41
10	Grassland	D,E	2.09	4.28	22
11	Savannah	D,E	1.66	3.61	41
12	Savannah	A,B,C	1.66	3.61	41
13	Grassland	A,B,C	2.09	4.28	22
14	Woody savannah	--	2.09	4.28	41
15	Mixed forest	--	1.29	2.8	13
16	Evergreen broadleaf forest	C,D,E	0.99	2.62	9
17	Deciduous broadleaf forest	C,D,E	1.16	2.42	11
18	Deciduous needle. forest	--	1.79	3.08	8.5
19	Evergreen needle. forest	--	1.76	4.18	8.5
20	Deciduous broadleaf forest	A,B	1.16	2.42	11
21	Evergreen broadleaf forest	A,B	0.99	2.62	9
22	Cropland	--	1.67	2.53	42.9
23	Urban and build-up lands	--	0	0	0
24	Cropland/nat. veg. mosaic	--	1.46	2.62	43.5

[c] A-equatorial, B-arid, C-warm temperature, D-snow, E-polar

Table A2 Mapping table to create the MODIS 24 soil biome map based on NLCD40 MODIS land cover categories for updated BDSNP parameterization

NLCD ID	NLCD40 MODIS CATEGORY (40)	MODIS ID	SOIL BIOME CATEGORY (24)
1	Evergreen Needle leaf Forest	19	Evergreen Needle leaf Forest
2	Evergreen Broadleaf Forest	16 and 21	Evergreen Broadleaf Forest
3	Deciduous Needle leaf Forest	18	Dec. Needle leaf Forest
4	Deciduous Broadleaf Forest	17 and 20	Dec. Broadleaf Forest
5	Mixed Forests	15	Mixed Forest
6	Closed shrublands	7	Closed shrublands
7	Open shrublands	8 and 9	Open shrublands
8	Woody Savannas	14	Woody savannah
9	Savannas	11 and 12	Savannah
10	Grasslands	10 and 13	Grassland
11	Permanent Wetlands	2	Permanent Wetland
12	Croplands	22	Cropland
13	Urban and Built Up	23	Urban and build-up lands
14	Cropland-Natural Vegetation Mosaic	24	Cropland/nat. veg. mosaic
15	Permanent Snow and Ice	3	Snow and ice
16	Barren or Sparsely Vegetated	6	Barren
17	IGBP Water	1	Water
18	Unclassified	4	Barren[d]
19	Fill value	5	Unclassified[d]
20	Open Water	1	Water
21	Perennial Ice-Snow	3	Snow and ice
22	Developed Open Space	23	Urban and build-up lands
23	Developed Low Intensity	23	Urban and build-up lands
24	Developed Medium Intensity	23	Urban and build-up lands
25	Developed High Intensity	23	Urban and build-up lands
26	Barren Land (Rock-Sand-Clay)	24	Cropland/nat. veg. mosaic
27	Unconsolidated Shore	24	Cropland/nat. veg. mosaic
28	Deciduous Forest	16 and 21	Evergreen Broadleaf Forest
29	Evergreen Forest	19	Evergreen Needle leaf Forest
30	Mixed Forest	15	Mixed Forest
31	Dwarf Scrub	8 and 9	Open shrublands
32	Shrub-Scrub	8 and 9	Open shrublands
33	Grassland-Herbaceous	10 and 13	Grassland
34	Sedge-Herbaceous	14	Woody savannah
35	Lichens	10 and 13	Grassland
36	Moss	10 and 13	Grassland
37	Pasture-Hay	24	Cropland/nat. veg. mosaic
38	Cultivated Crops	22	Cropland
39	Woody Wetlands	2	Permanent Wetland
40	Emergent Herbaceous Wetlands	2	Permanent Wetland

[d] NLCD categories 18 and 19 were mapped as MODIS category 1 (Water) in Rasool et al. (2016), which have been corrected here.

Table A3 Microbial/Organic biomass C and N % and HONO/N_{NOx} % mapped to respective NLCD40 MODIS land-cover categories based on Xu et al. (2013) estimates

NLCD ID	NLCD40 MODIS CATEGORY (40)	Cmic %	Nmic %	$HONO_f$ %
1	Evergreen Needle leaf Forest	1.76	4.18	8.5
2	Evergreen Broadleaf Forest	0.99	2.62	9
3	Deciduous Needle leaf Forest	1.79	3.08	8.5
4	Deciduous Broadleaf Forest	1.16	2.42	11
5	Mixed Forests	1.29	2.80	13
6	Closed shrublands	1.43	2.33	35.5
7	Open shrublands	1.43	2.33	41
8	Woody Savannas	2.09	4.28	41
9	Savannas	1.66	3.61	41
10	Grasslands	2.09	4.28	22
11	Permanent Wetlands	1.2	2.58	0
12	Croplands	1.67	2.53	42.9
13	Urban and Built Up	0	0	0
14	Cropland-Natural Vegetation Mosaic	1.46	2.62	43.5
15	Permanent Snow and Ice	0	0	0
16	Barren or Sparsely Vegetated	5.02	5.72	48
17	IGBP Water	0	0	0
18	Unclassified	5.02	5.72	48
19	Fill value	0	0	0
20	Open Water	0	0	0
21	Perennial Ice-Snow	0	0	0
22	Developed Open Space	0	0	0
23	Developed Low Intensity	0	0	0
24	Developed Medium Intensity	0	0	0
25	Developed High Intensity	0	0	0
26	Barren Land (Rock-Sand-Clay)[e]	0	0	0
27	Unconsolidated Shore[e]	0	0	0
28	Deciduous Forest	0.99	2.62	9
29	Evergreen Forest	1.76	4.18	8.5
30	Mixed Forest	1.29	2.8	13
31	Dwarf Scrub	1.43	2.33	41
32	Shrub-Scrub	1.43	2.33	41
33	Grassland-Herbaceous	2.09	4.28	22
34	Sedge-Herbaceous	2.09	4.28	41
35	Lichens	2.09	4.28	22
36	Moss	2.09	4.28	22
37	Pasture-Hay[f]	0	0	43.5
38	Cultivated Crops[f]	0	0	42.9
39	Woody Wetlands	1.2	2.58	0
40	Emergent Herbaceous Wetlands	1.2	2.58	0

[e] NLCD classes 26 and 27 constituting of rocks mostly. [f] Cmic and Nmic for US croplands classified under NLCD classes 37 and 38 are kept as zero to prevent double counting, as they are accounted for by EPIC N data.